THE ASTROPHYSICAL JOURNAL, 311:843–863, 1986 December 15

THE CHEMICAL COMPOSITION OF RED GIANTS. II. HELIUM BURNING AND THE *s*-PROCESS IN THE MS AND S STARS

VERNE V. SMITH[1] AND DAVID L. LAMBERT[1]
Department of Astronomy, University of Texas, and McDonald Observatory
Received 1986 March 14; accepted 1986 May 21

ABSTRACT

Carbon, nitrogen, oxygen, Fe-peak, and heavy *s*-process elemental abundances have been determined for an additional 12 stars of type M, MS, or S. When combined with results obtained previously for nine stars of type M or MS and the K5 giant α Tau (Smith and Lambert 1985, hereafter Paper I), abundances are available for 22 cool red giants. These abundances are derived from high-resolution, high signal-to-noise (S/N) digital spectra in the infrared and near-infrared. Abundances based upon atomic lines are referenced to the comparison giant, α Tau, to minimize non–LTE effects and the CNO abundances are based on molecular lines from CO, OH, NH, and CN. In addition, Mg-isotopic ratios and technetium abundances are estimated for selected stars.

Of the 22 stars studied, eight are of type MS and three of type S. Four of the MS stars show no measurable enhancements of the *s*-process elements and have CNO abundances that are consistent with their being first dredge-up giants similar to α Tau and the M stars (i.e., reduced ^{12}C and enhanced ^{14}N).

The seven stars which exhibit *s*-process enhancements also show increasing ^{12}C abundances (the result of ^4He-burning) and the ^{12}C abundances correlate with both absolute *s*-process enhancement and integrated neutron exposure. No enhanced ^{25}Mg abundances are seen in the *s*-process enriched stars, ruling out $^{22}Ne(\alpha, n)^{25}Mg$ as the probable neutron-source for the *s*-process in these stars. The competing reaction, $^{13}C(\alpha, n)^{16}O$, is the presumed neutron source. Estimates of the Tc abundance indicate that some of the stars have been in the thermally pulsing, asymptotic giant branch (AGB) phase of evolution for nearly 10^6 yr.

The results for the *s*-process and ^{12}C-rich stars are compared to theoretical models of low-mass ($M \approx 1$–$2\ M_\odot$), thermally pulsing AGB stars.

Subject headings: nucleosynthesis — stars: abundances — stars: late-type

I. INTRODUCTION

Isolation of S stars as a group outside the Harvard types M and N is attributable to Merrill (1922). Thirty years later, his discovery (Merrill 1952) of unstable technetium in red giants, primarily of type S, provided both incontrovertible evidence of recent, even continuing, nucleosynthesis in these stars and a stimulus for a theoretical attack on stellar nucleosynthesis. Today, the theoretical understanding of nucleosynthesis in stars on the asymptotic giant branch (AGB) is advancing rapidly. Our purpose is to provide detailed information on the chemical composition of S and the related MS stars and to examine the results in the light of current theoretical predictions.

Keenan (1954) classified S stars according to the ratio of ZrO to TiO band strengths and introduced the intermediate type of MS stars having much weaker ZrO than the S stars; at classification dispersions, absence of ZrO is a mark of M giants. A class, intermediate between S and the N-type carbon stars, was described by Bidelman (1954) and termed SC (i.e., both ZrO and C_2 weakly present). The sequence M-MS-S-SC-C is now thought to be one of increasing carbon to oxygen ratio with the transition from C/O < 1 to C/O > 1 occurring within the SC type. The role of the C/O ratio reflects the controlling influence of the CO molecule on the partial pressures of free C and O, a point emphasized by Russell (1934).

The progressive enhancement of carbon and those elements synthesized via neutron capture in the *s*-process (e.g., Tc and the Zr shown by Boesgaard [1970] to be enhanced in MS and S stars) is now attributed to a thermal instability of the He-burning shell of the AGB star (Schwarzschild and Härm 1965). Modeling of these instabilities, or thermal pulses, in intermediate mass stars predicts enhancements of surface ^{12}C and *s*-process elements such that the AGB star of type M is converted to an N-type carbon star (Iben 1975; Truran and Iben 1977; Iben and Truran 1978). Recent theoretical work suggests that a similar dredge-up from the He-burning shell may occur in lower mass stars (Iben and Renzini 1982; Iben 1983).

Observational tests of the theoretical models call for abundance analyses covering those elements and isotopes influenced by the dredge-up. In particular, analyses should include the key monitors of H- and He-burning zones (C, N, O), an indicator of the overall metallicity of the stars (the Fe group), and various heavy elements sensitive to the *s*-process. Spectroscopists limited to the visual spectrum are hampered by severe molecular line blanketing by molecular bands, and the signatures of C, N, and O are incomplete in this region. Access to the less-blanketed near-infrared and to the infrared, the domain of transitions from C, N, and O containing molecules, is a prerequisite to an adequate abundance analysis. In Paper I of this series, we analyzed a sample of M and MS giants (Paper I). Here, we expand the sample by a further 12 stars: four are normal M stars, six were classified as MS stars by Yamashita (1967), and two are well-known S stars (HR 1105 and HR 8714). When the reclassifications suggested by our analyses are made, the combined sample of 21 stars comprises

[1] Visiting Astronomer, Kitt Peak National Observatory, National Optical Astronomy Observatories, Operated by the Association of Universities for Research in Astronomy, Inc., under contract with the National Science Foundation.

14 M, four MS, and three S stars. Spectroscopic coverage employed in Paper I is extended here to observations of the Tc I resonance lines and MgH lines in selected stars.

II. OBSERVATIONS

High-resolution spectra of the stars listed in Table 1 were obtained using the McDonald Observatory's 2.7 m telescope, coudé spectrograph and Reticon array (Vogt, Tull, and Kelton 1978) and the Kitt Peak National Observatory's (KPNO) 4 m telescope and Fourier Transform Spectrometer (FTS; Hall *et al.* 1978). The Reticon spectra have a resolution of 0.2 Å at 7500 Å and the FTS spectra were obtained with a typical resolution of 0.05 cm^{-1}. The wavelengths of the near-IR spectra were chosen to avoid molecular line-blanketing and consist of spectra from 7400–7580 Å and 9980–10,100 Å. These regions are relatively uncrowded and permit accurate determinations of equivalent widths in stars as late as type M6. Three spectral windows near wavelengths of 1.6 μm, 2.2 μm, and 4.0 μm were observed with the KPNO FTS. Telluric-line contamination of the spectra was minimized by dividing the spectrum with that of a hot star. Molecular lines from C, N, and O carrying molecules are present on the FTS spectra. The 1.6 μm region contains OH ($\Delta v = 2$) and CO ($\Delta v = 3$) vibration-rotation ($V-R$) lines, while near 2.2 μm we employ CO ($\Delta v = 2$) $V-R$ lines and CN ($\Delta v = 2$) red system lines ($A\ ^2\Pi$–$X\ ^2\Sigma$). The spectral window near 4.0 μm contains OH ($\Delta v = 1$) $V-R$ lines.

Figure 1 illustrates sample McDonald spectra near 7450 Å for three types of stars; an M giant (μ Gem), an MS star (10 Dra) and an S star (HR 1105). The temperatures of all three stars are similar, but note a comparison of the strengths of the Zr I and Y II lines relative to the Fe I lines. The Zr I and Y II lines are obviously strengthened in the S star, HR 1105, but not notably enhanced in the MS star, 10 Dra, relative to the M giant, μ Gem. Indeed, not all of the stars classified as MS by Yamashita (1967) show measurable enhancements of the *s*-process elements. We find that out of nine stars classified as MS by Yamashita (1967) and observed by us, five show definite *s*-process enhancements and one of these five shows abundances more typical of an S star.

Figure 2 shows a region of spectrum in the 4 μm window for the S star HR 1105. Also shown is the comparison spectrum from IRC + 10216, a heavily obscured carbon star which shows no spectral features in this region; hence, the features in its spectrum are telluric lines. A ratioed spectrum of HR 1105/IRC + 10216 is illustrated at the bottom with fundamental $V-R$ lines from OH and NH indicated. The NH lines are unresolved triplets with components as indicated below the spectrum.

In addition to the near-IR and IR observations, spectra were obtained in heavily blanketed regions in the violet and green regions of the spectrum in order to extract information on the presence of the unstable element technetium and magnesium isotopic ratios via the MgH lines. Merrill (1922, 1952) first detected evidence for technetium in late-type stars (primarily of type S) through the three permitted resonance lines of Tc I near 4250 Å. We observed this region using the McDonald Reticon at 0.2 Å resolution. The MgH lines were observed near 5140 Å and consist of (0, 0) and (1, 1) lines from the $A\ ^2\Pi$–$X\ ^2\Sigma$ system which provide the $^{24}Mg/^{25}Mg/^{26}Mg$ ratios. The McDonald Reticon was used with an echelle grating giving a resolution of 0.05 Å.

III. ANALYSIS

Since the analysis is patterned after that of Paper I, a brief review suffices. The model atmospheres are from Johnson, Bernat, and Krupp (1980). Effective temperatures are determined from broad-band colors and the calibrations by Ridgway *et al.* (1980) for ($V-K$), Tsuji (1981) for ($R-I$), and McWilliam and Lambert (1984) for the IR color ($J-K'$). Temperatures derived for the same star from different colors are in excellent agreement, a difference of 100 K or less is typical.

As in Paper I, stellar surface gravities were calculated from estimates of M_{bol} and T_{eff} along with stellar masses obtained by comparison with evolutionary model tracks in a log $L/L_\odot$–log T_{eff} plane. Figure 3 shows a modified version of the HR Diagram for the stars in our sample along with first-ascent red-giant models from Paczyński (1970) and Sweigart and Gross (1978) and models of thermally pulsing AGB stars from Becker and Iben (1979). The error bar corresponds to an

TABLE 1

BASIC STELLAR QUANTITIES

HR Number	Name	Spectral Type[a]	$(V-K)$[b]	$(R-I)$[b]	$(J-K')$[c]	M_v[d]	M_{bol}[e]
921.....	ρ Per	M4+IIIa	5.32	1.62	...	−0.8	−3.2
1105.....	BD Cam	S5, 3	...	1.39	...	−0.8	−3.4
2286.....	μ Gem	M3+IIIa	4.76	1.38	1.17	−0.7	−2.6
2508.....	...	M2 IIabS	...	...	...	−2.1	−3.9
3639.....	RS Cnc	M6 IIIaS	...	2.33	1.32	...	−5.5[f]
4088.....	44 Leo	M2+IIIabS	...	...	1.09	+0.1	−1.5
4483.....	ω Vir	M4+IIIab	...	...	1.19	+0.2	−2.6
5226.....	10 Dra	M3 IIIaS	4.75	1.36	1.12	−0.6	−2.5
7405.....	α Vul	M1 IIIab	3.90	0.97	1.02	−0.5	−1.8
7442.....	...	M5−IIIaS	...	...	1.20	...	−4.0[f]
8062.....	...	M4 IIIaS	...	1.56	...	...	−3.5[f]
8714.....	HR Peg	S5, 3	...	1.46	...	...	−3.3[g]

[a] Yamashita 1967.
[b] Johnson *et al.* 1966.
[c] McWilliam and Lambert 1984.
[d] Wilson (1976) or Yamashita 1967.
[e] Bolometric corrections to M_v using Bessell and Wood 1984, except where noted.
[f] Estimated from spectral type.
[g] Eggen 1972.

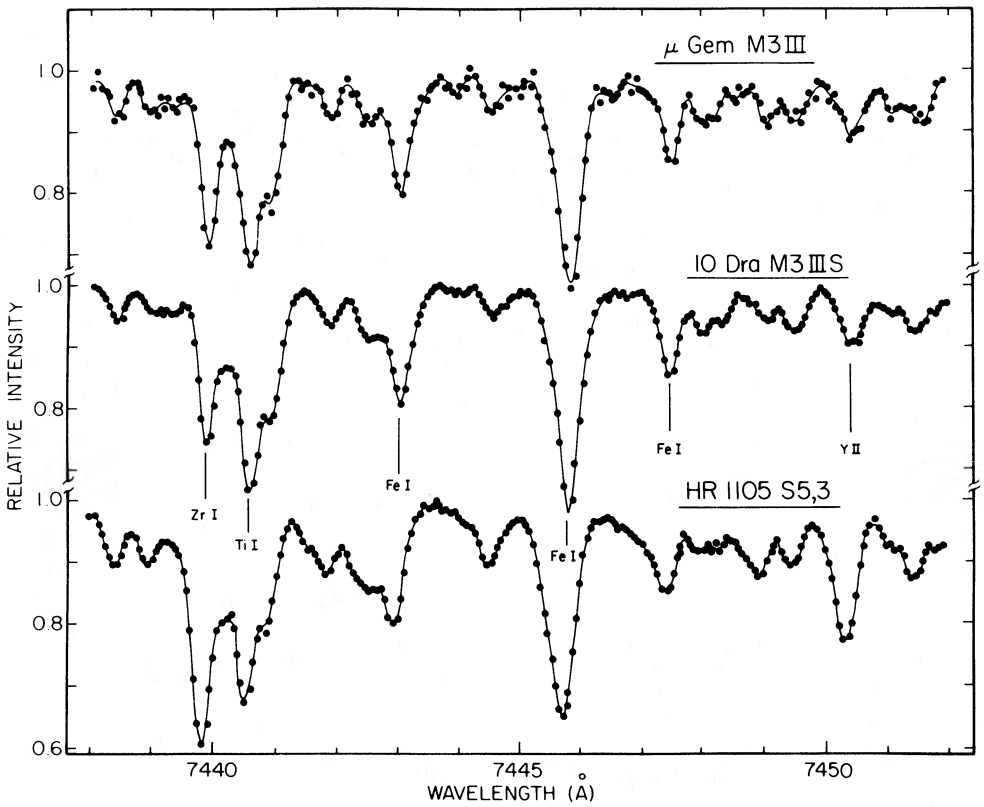

FIG. 1.—Sample McDonald Reticon spectra near 7450 Å for an M, MS, and S star

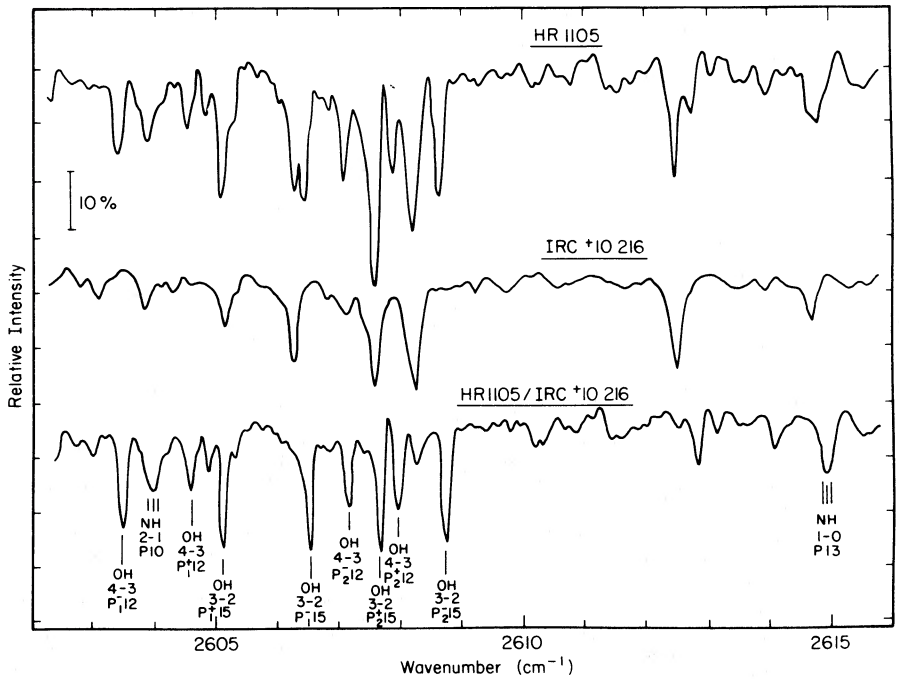

FIG. 2.—Sample Kitt Peak FTS spectra showing an S star (HR 1105), telluric absorption (IRC+10216) and the resultant ratio which minimizes telluric contamination.

TABLE 2

DERIVED STELLAR PROPERTIES

Star	$T_{\rm eff}$(K)	log g	ξ (km s^{-1})
ρ Per	3500	0.8	1.8
HR 1105	3550	0.9	2.0
μ Gem	3600	1.0	1.9
HR 2508	3600	0.7	3.1
RS Cnc	3200	0.0	2.5
44 Leo	3700	1.4	2.2
ω Vir	3450	0.8	2.0
10 Dra	3650	1.0	1.8
α Vul	3850	1.4	1.8
HR 7442	3450	0.5	1.9
HR 8062	3450	0.7	1.9
HR 8714	3500	0.9	2.1

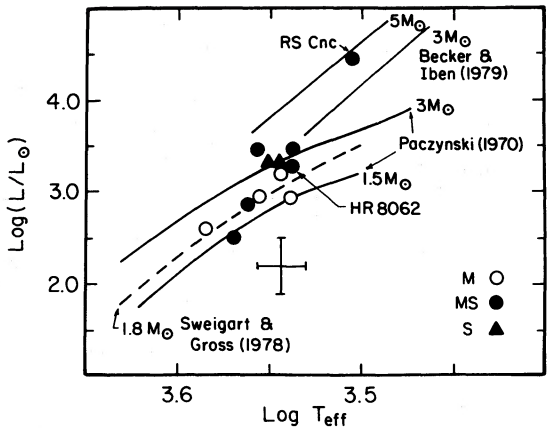

FIG. 3.—Derived luminosities and effective temperatures of red giants in this study are shown along with model evolutionary tracks of different-mass stars from several investigators.

uncertainty in luminosity of, plus or minus, a factor of 2 and an uncertainty in $T_{\rm eff}$ of ± 100 K. Our selection largely comprises low- to intermediate-mass stars (1–5 $M_\odot$). The two MS stars identified in Figure 3, RS Cnc and HR 8062, show definite *s*-process enhancements according to our analysis. The remaining four stars, although classified MS by Yamashita (1967), do not show measurable *s*-process overabundances (within the uncertainties of our analysis). Table 2 lists the model parameters.

A standard LTE analysis was performed using a sample of molecular and atomic lines. We use the basic LTE analysis code from Sneden (1974). The atomic-line list and measured equivalent widths are listed in Table 3. As in Paper I, all abundances derived from atomic lines are relative to the K5 giant α Tau in order to minimize non–LTE effects seen in cool giants (Ruland *et al.* 1980; Brown, Tomkin, and Lambert 1983; Tomkin and Lambert 1983). Microturbulent velocities (ξ; see Table 2) are determined from the Fe I, Ni I, and Ti I lines by requiring that the derived abundances be independent of equivalent width; the microturbulent velocities are accurate to ± 0.3 km s^{-1}.

Tables 4 and 5 present a selection of the weaker $^{12}C^{16}O$ (hereafter ^{12}CO) equivalent widths (in millikaysers) for the

TABLE 3

ATOMIC LINE LIST

Species	λ (Å)	χ (eV)	Equivalent Width (mÅ) ρ Per	HR 1105	μ Gem	HR 2508	RS Cnc	44 Leo	ω Vir	10 Dra	α Vul	HR 7442	HR 8062	HR 8714
Ti I	7474.94.....	1.75	103	118	108	133	133	107	123	102	81	124	124	116
	7496.12.....	2.24	119	127	119	164	...	110	120	109	95	133	130	119
	9997.94.....	1.87	..	138	148	199	162	121	147	145	...	162	162	155
	10003.02.....	2.15	126	107	123	170	141	103	117	134	...	138	135	123
	10034.55.....	1.45	225	196	183	264	235	169	196	190	...	225	210	210
Fe I	7447.43.....	4.95	55	66	62	94	115	74	66	52	58	71	62	56
	7477.52.....	3.88	53	...	61	68	...	65	69	53	40	70	61	46
	7507.30.....	4.41	88	109	99	161	122	102	82	88	107	104	109	106
	7540.44.....	2.73	75	83	83	150	...	92	83	67	69	102	91	87
	7559.68.....	5.06	...	...	...	112	...	74	54	50	53	...	...	...
	7583.80.....	3.02	190	162	158	245	219	181	176	149	145	166	162	162
	10065.08.....	4.81	92	88	90	142	73	95	75	92	...	88	88	92
Ni I	7385.24.....	2.75	97	...	117	186	128	115	112	105	112	114	112	109
	7393.63.....	3.61	117	135	126	208	...	148	135	124	138	123	126	126
	7414.51.....	1.99	166	174	166	257	214	196	108	122	149	200	186	178
	7422.30.....	3.63	126	145	138	224	...	166	124	121	126	159	132	135
	7522.78.....	3.66	114	131	137	...	157	161	144	120	148	143	137	150
	7525.14.....	3.63	86	106	104	193	99	123	94	96	109	114	111	114
	7574.08.....	3.83	93	109	100	170	...	124	112	98	93	115	109	98
Sr II	10036.65.....	1.80	178	241	152	303	276	122	165	152	...	191	210	210
Y II	7450.32.....	1.74	38	110	48	108	118	53	55	40	39	59	84	86
Zr I	7439.89.....	0.54	98	163	113	174	215	99	114	96	71	129	145	155
	7553.00.....	0.51	44	117	42	83	137	44	50	37	33	70	95	83
	7554.73.....	0.51	95	154	100	125	208	75	110	85	56	125	144	134
	7558.41.....	1.54	29	89	30	52	97	26	35	21	15	50	60	54
Ba I	7392.41.....	1.57	13	52	16	...	50	15	10	13	11	21	22	25
Nd II	7513.73.....	0.92	43	79	52	62	111	22	35	30	28	53	60	58

TABLE 4

^{12}CO First-Overtone Vibration-Rotation Lines

Line	σ (cm^{-1})	χ (eV)	log gf	W_σ(cm^{-1}) × 10^3 HR 1105	HR 2508	RS Cnc	44 Leo	ω Vir	10 Dra	α Vul	HR 7442	HR 8062	HR 8714
2–0 Band													
R94.....	4285.21	2.07	−4.84	61	...	...	...	33	46	...	...	...	60
R92.....	4292.04	1.98	−4.85	59	55	66	39	48	45	46	47	50	62
R81.....	4323.69	1.55	−4.93	82	78	91	61	72	63	68	70	73	82
R80.....	4326.07	1.51	−4.94	82	84	93	61	77	67	62	72	75	82
R79.....	4328.37	1.48	−4.95	84	87	97	70	79	72	67	75	82	86
R78.....	4330.58	1.44	−4.95	86	89	99	69	78	74	61	77	83	88
R77.....	4332.72	1.40	−4.96	84	87	99	66	77	72	55	77	79	88
3–1 Band													
R63.....	4299.00	1.21	−4.61	116	139	136	98	100	93	...	101	111	121
R37.....	4298.74	0.60	−4.90	156	...	162	124	140	131	134	133	...	...
R32.....	4292.75	0.51	−4.98	159	182	168	127	140	137	128	139	152	...

$\Delta v = 2$ and 3 $V-R$ lines, respectively. Values of ξ derived from the ^{12}CO lines are in agreement with those derived from the atomic lines. The very strong ^{12}CO lines (log $W_\sigma/\sigma \gtrsim -4.2$) tend to give larger abundances. Since the line cores of such strong lines are saturated in the first layer of the model atmosphere, these strong lines are unreliable as abundance indicators. Such lines could be used to develop an empirical model for the upper photosphere and low chromosphere. The ^{13}CO lines used to determine ^{13}C-abundances (and hence ^{12}C/^{13}C ratios) are listed in Table 6.

The ^{16}OH lines and equivalent widths are shown in Table 7 ($\Delta v = 1$) and Table 8 ($\Delta v = 2$). The first-overtone lines are the same ones used in Paper I while the fundamental lines are new to the present study. Oscillator strengths for both series of OH lines are based upon transition probabilities from van Dishoeck (1985). RS Cnc and 44 Leo are omitted from Tables 7 and 8. Both stars were observed in the 4 μm window to obtain the $\Delta v = 1$ ^{16}OH $V-R$ lines; however, for different reasons both spectra were unusable. In the case of 44 Leo, the spectrum was very noisy (S/N < 10) while for RS Cnc it was noticed that all lines in the region (including SiO and NH) were much weaker than expected for such a late-type star (M6). Spectrophotometry of RS Cnc (Merrill and Stein 1976) shows an IR-excess at 4 μm. This excess, which "fills in" the absorp-

TABLE 5

^{12}CO Second-Overtone Vibration-Rotation Lines

Line	σ (cm^{-1})	χ (eV)	log gf	W_σ(cm^{-1}) × 10^3 ρ Per	HR 1105	μ Gem	α Vul	HR 8714
3–0 Band								
P36.....	6147.00	0.32	−7.88	56	77	...	35	95
4–1 Band								
P19.....	6181.02	0.36	−7.47	73	79	69	46	102
P18.....	6186.70	0.35	−7.49	76	76	65	52	103
5–2 Band								
P14.....	6129.82	0.58	−7.16	70	77	57	50	98
P13.....	6134.95	0.57	−7.19	70	81	66	41	104
P10.....	6149.71	0.55	−7.29	66	84	56	40	112
6–3 Band								
R63.....	6127.88	1.71	−5.80	...	50	...	40	70
R60.....	6137.37	1.63	−5.84	66	78	...	47	...
R59.....	6140.30	1.60	−5.85	63	64	49	41	91
R41.....	6173.79	1.18	−6.09	78	80	69	58	112
R20.....	6167.39	0.88	−6.50	87	111	83	70	131
R18.....	6164.28	0.87	−6.55	...	94	...	62	117
R17.....	6162.56	0.86	−6.58	91	89	83	60	111
R16.....	6160.73	0.85	−6.61	87	100	...	68	109
R15.....	6158.79	0.84	−6.64	74	90	81	52	112
R14.....	6156.75	0.84	−6.67	81	84	78	54	103
R8	6142.25	0.80	−6.92	66	67	56	42	92
R6	6136.56	0.80	−7.04	60	...	...	41	...
R4	6130.45	0.79	−7.20	...	53	...	31	79

TABLE 6

^{13}CO VIBRATION-ROTATION LINES

LINE	σ (cm^{-1})	χ (eV)	log gf	W_σ(cm^{-1}) × 10^3										
				ρ Per	HR 1105	μ Gem	HR 2508	RS Cnc	44 Leo	ω Vir	10 Dra	α Vul	HR 7442	HR 8062	HR 8714
4–1 Band															
R47.....	6193.57	0.77	−6.69	18	13	15	...	...	...	...	...	13	...	...	12
R23.....	6194.26	0.38	−7.13	17	13	18	...	...	...	...	...	15	...	...	13
5–2 Band															
R51.....	6110.38	1.11	−6.22	16	10	14	...	...	...	...	...	12	...	...	8
R48.....	6115.08	1.04	−6.26	12	8	12	...	...	...	...	...	10	...	...	8
R18.....	6110.81	0.59	−6.84	17	14	23	...	...	...	...	...	14	...	...	12
2–0 Band															
R71.....	4251.23	1.15	−5.01	...	45	...	50	67	...	40	55	...	41	36	...
R70.....	4252.61	1.12	−5.01	...	45	...	39	48	42	40	45	...	39	33	...
R69.....	4253.91	1.08	−5.02	...	42	...	50	60	...	52	49	61	44	40	52
R68.....	4255.14	1.05	−5.03	...	46	...	52	54	49	52	52	...	47	44	50
R64.....	4259.30	0.94	−5.07	...	44	...	50	47	48	45	46	54	45	33	55
R61.....	4261.64	0.85	−5.10	...	50	...	62	56	55	57	61	61	51	46	67
R43.....	4261.89	0.43	−5.30	...	69	...	85	72	61	78	76	74	68	59	69
R41.....	4260.48	0.39	−5.33	...	72	...	86	68	70	77	73	68	71	62	77
R40.....	4259.67	0.37	−5.34	...	79	...	85	68	88	83	81	...	72	61	80
R38.....	4257.83	0.34	−5.37	...	72	...	86	71	...	82	86	78	71	67	...
R37.....	4256.81	0.32	−5.38	...	72	...	90	77	82	86	82	...	75	69	84
R33.....	4252.00	0.25	−5.44	...	81	...	93	78	...	87	105	...	81	73	...

TABLE 7

^{16}OH FUNDAMENTAL VIBRATION-ROTATION LINES

LINE	σ (cm^{-1})	χ (eV)	log gf	W_σ (cm^{-1}) × 10^3						
				ρ Per	HR 1105	μ Gem	HR 2508	ω Vir	10 Dra	HR 7442	HR 8062
3–2 Band											
P_1^+17.5.....	2505.27	1.50	−3.74	41	...	25	36	26	25	35	36
15.5.....	2605.13	1.36	−3.84	...	26	30	35	31	35	40	34
14.5.....	2655.31	1.30	−3.90	...	...	30	37	31	31	37	30
P_1^-17.5.....	2506.82	1.49	−3.74	43	...	26	32	25	30	33	36
15.5.....	2606.50	1.36	−3.84	38	...	32	...	27	33	41	31
14.5.....	2653.98	1.30	−3.90	33	39	31	37	27	...	...	...
P_2^+16.5.....	2507.43	1.50	−3.71	...	...	22	...	30	40	...	...
14.5.....	2607.69	1.37	−3.81	...	...	29	31	...	32	41	31
13.5.....	2657.78	1.30	−3.87	32	...	32	38	...	30	39	32
P_2^-16.5.....	2508.65	1.50	−3.71	40	25	25	29	25	...	38	32
14.5.....	2608.81	1.37	−3.81	...	...	29	32	30	34	...	35
13.5.....	2656.79	1.31	−3.87	38	40	31	39	29	32	37	...
4–3 Band											
P_1^+12.5.....	2604.55	1.58	−4.05	26	19	23	22	20	22	25	26
11.5.....	2648.56	1.53	−4.13	...	18	22	21	20	27	...	...
10.5.....	2693.29	1.49	−4.21	36	25	...	19	24	26	26	...
P_1^-12.5.....	2603.51	1.58	−4.05	28	...	20	25	22	23	24	...
11.5.....	2649.43	1.53	−4.13	...	...	23	...	...	27	28	22
10.5.....	2692.43	1.49	−4.21	35	...	17	20	22	26	23	27
P_2^+11.5.....	2607.91	1.58	−4.01	...	24	...	24	21	25	24	30
10.5.....	2652.61	1.54	−4.08	34	21	20	19	20	27	31	22
9.5.....	2697.80	1.49	−4.16	33	17	18	22	20	25	...	21
P_2^-11.5.....	2607.22	1.58	−4.01	...	23	19	...	19	23	...	28
10.5.....	2653.12	1.54	−4.08	30	21	19	23	22	27	27	...
9.5.....	2697.09	1.49	−4.16	...	22	20	...	27	23	27	21

TABLE 8

^{16}OH First-Overtone Vibration Lines

Line	σ (cm^{-1})	χ (eV)	log gf	W_σ(cm^{-1}) × 10^3				
				ρ Per	HR 1105	μ Gem	α Vul	HR 8714
2–0 Band								
P_1^+21.5.....	5680.60	1.01	−4.90	88	73	83	68	94
P_1^-21.5.....	5683.44	1.01	−4.90	...	77	90	69	99
18.5.....	5848.22	0.84	−5.01	106	102	110	78	...
P_2^+20.5.....	5682.68	1.02	−4.94	91	83	89	76	100
19.5.....	5767.44	0.93	−4.97	113	...	98	85	113
3–1 Band								
P_1^+15.5.....	5842.85	0.96	−4.64	122	111	108	...	122
P_1^-15.5.....	5844.75	0.96	−4.64	128	93	105	89	121
P_2^+16.5.....	5700.69	1.10	−4.60	120	...	109	87	...
P_2^-16.5.....	5702.30	1.10	−4.60	117	91	104	77	106
14.5.....	5847.59	0.96	−4.69	109	97	112	89	116
4–2 Band								
P_1^+12.5.....	5737.69	1.19	−4.47	91	76	88	72	92
P_1^-12.5.....	5736.26	1.19	−4.47	97	78	74	68	97
P_2^+10.5.....	5801.94	1.15	−4.59	101	92	106	81	102
9.5.....	5863.48	1.10	−4.65	103	93	100	84	127
P_2^-10.5.....	5803.79	1.15	−4.59	...	...	99	78	...
9.5.....	5862.75	1.10	−4.65	105	...	98	89	127
5–3 Band								
P_1^+7.5.....	5704.35	1.38	−4.56	77	56	64	49	62
6.5.....	5752.78	1.35	−4.65	76	59	63	46	75
4.5.....	5840.04	1.31	−4.86	74	63	53	40	79
P_1^-7.5.....	5705.01	1.38	−4.56	84	...	74	...	...
6.5.....	5752.15	1.35	−4.65	83	67	66	53	77
P_2^-6.5.....	5714.06	1.39	−4.65	76	...	84	61	...

tion lines, renders the 4 μm spectrum unusable. Fortunately, the spectrophotometry extends down to 2 μm and shows quite clearly that the excess begins near 3.2 μm while the 2 μm region in RS Cnc is apparently unaffected.

A limitation on the ^{16}OH ($\Delta v = 1$) $V-R$ lines was noticed in our analysis. Lines from the (1–0) and (2–1) bands gave much higher ^{16}O abundances (up to 0.6 dex) than the (3–2) or (4–3) lines and the lines from the $\Delta v = 2$ transitions. Although the (3–2) and (4–3) lines are weaker than those from the (1–0) and (2–1) bands, the discrepancy cannot be attributable solely to saturation effects because some of the $\Delta v = 2$ lines are as strong as the discrepant 1–0 and 2–1 lines. We suspect that the cores of the strong 1–0 and 2–1 lines are formed in the outermost layers of the atmosphere where structure cannot be predicted satisfactorily. A similar effect was noticed by Lambert *et al.* (1984) in their analysis of α Ori. Here, we restrict our analysis to the (3–2) and (4–3) bands, and the first overtone $V-R$ lines of OH.

The combination of CO and OH allows a determination of both C and O abundances. For these oxygen-rich stars, the CO density is set almost entirely by the C abundance. The formation of OH is set by the abundance difference (O−C). In Figure 4 is shown a determination of the C and O abundances for the S star HR 1105. Two loci are plotted; one shows the carbon abundance derived from the ^{12}CO (and ^{13}CO) lines as a function of an assumed oxygen abundance. The other loci shows the oxygen abundance derived from OH lines as a function of the assumed total carbon abundance. The intersection of these two loci provides the C and O abundances. For HR 1105 we see that log ϵ(C) ≈ 8.75 and log ϵ(O) ≈ 8.92, indicating a slight increase in C/O over the solar ratio.

Nitrogen abundances were derived from the two N-bearing molecules CN and NH. The lines from CN (Table 9) are the same ones as in Paper I. The NH transitions and equivalent widths are shown in Table 10. Each feature is a triplet. Our NH lines were included in the α Ori analysis by Lambert *et al.* (1984). For each of the unresolved triplets (see Fig. 2), we predicted equivalent widths from a spectrum synthesis using accurate frequency splittings provided by Bernath (1985). We adopt

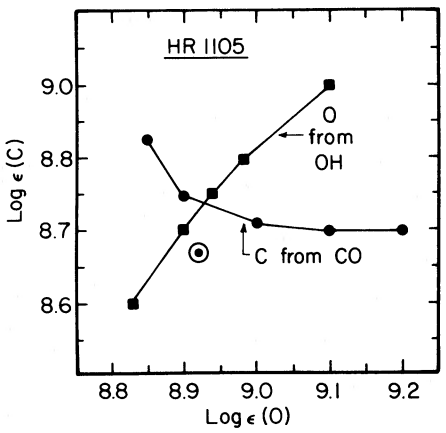

FIG. 4.—Abundance solutions for CO and OH for the S star HR 1105. The solar C and O abundance is indicated.

TABLE 9

2μm $^{12}C^{14}N$ RED SYSTEM LINES

LINE	σ (cm^{-1})	χ (eV)	log gf	$W_\sigma(cm^{-1}) \times 10^3$ HR 1105	HR 2508	RS Cnc	44 Leo	ω Vir	10 Dra	α Vul	HR 7442	HR 8062	HR 8714
0–2 Band													
$P_1$47.....	4558.98	1.02	−2.27	23	15	20	8	17	9	12	14	18	30
$P_2$24.....	4586.63	1.00	−2.29	26	16	27	9	15	14	12	14	25	35
$Q_1$57.....	4563.90	1.26	−1.70	26	18	...	13	21	12	...	13	25	...
1–3 Band													
$Q_2$44.....	4567.15	1.20	−1.69	32	25	27	14	22	22	14	17	26	36
$Q_2$45.....	4553.77	1.22	−1.68	29	25	26	13	22	20	13	18	27	35
2–4 Band													
$Q_1$19.....	4587.28	1.08	−1.90	...	24	...	26	21	21	13	19	...	...
$Q_1$23.....	4563.16	1.12	−1.81	26	22	26	14	20	14	16	15	25	34
$Q_2$26.....	4558.03	1.15	−1.77	26	21	24	14	21	17	...	15	22	33
$R_2$39.....	4560.60	1.34	−1.86	23	15	18	7	17	12	9	10	18	19

the *gf*-values used by Lambert *et al.* (1984). The advantage of NH over CN is, of course, the independence of the nitrogen abundances derived using NH from the carbon abundance.

The results of our LTE analysis are presented in Table 11. This is a sister table to Table 5 of Paper I. The C, N, and O abundances are presented on an absolute scale. The atomic abundances are given relative to the standard star, α Tau, in standard spectroscopic bracket notation:

$$[X/H] = \log_{10}(X/H)_{\text{program star}} - \log_{10}(X/H)_{\text{standard star}} .$$

Quoted uncertainties for some entries are standard deviations in the derived abundances from the sample of lines used in the analysis (obviously no such quantity can be defined for abundances based upon single lines). Sensitivities to various model atmosphere parameters (T_{eff}, log g, ξ) for each species were given in Table 4 of Paper I and are not repeated here.

An examination of Table 11 reveals a curious feature involving the *s*-process elements (Y, Zr, Ba, and Nd; Sr-abundances should be viewed with caution because of systematic trends in the Sr II line discussed in § IV) in the MS stars. Not all MS stars show measurable enhancement of the *s*-process elements. In fact, of the six MS stars included here, only two (RS Cnc and HR 8062) exhibit distinct enhancements of [*s*-process/Fe]. It is possible that our analyses are insufficiently sensitive to detect very slight ([*s*-process/Fe] $\lesssim +0.2$) enhancements. A review of Yamashita's (1967) comments concerning the four, apparently normal, MS stars (HR 2508, 44 Leo, 10 Dra, and HR 7442) is enlightening. In three of the stars (44 Leo, 10 Dra, and HR 7442), the λ4554 Ba II line is listed as only "slightly enhanced" while in 44 Leo and 10 Dra, ZrO is also only "slightly enhanced." As the classification system depends upon a comparison to a standard star, very slight differences due to temperature, luminosity, chemical composition, or microturbulence could lead to small differences in the visual appearance of the spectrum, i.e., small changes in a very strong line such as Ba II or the faint appearance of ZrO. Zirconium oxide is definitely enhanced in HR 7442 but so are VO, ScO, and YO. Perhaps the temperature classification of HR 7442 should be lowered. The Ba II line is listed as "greatly enhanced" in HR 2508, with ZrO and YO enhanced slightly. A reexamination of Table 2 reveals that HR 2508 has a microturbulent velocity almost 1 km s^{-1} larger than the typical giant; hence, the presence of an "enhanced" strong line is not surprising. Indeed, a visual inspection of the high-resolution spectrum reveals the extreme microturbulent velocity. The weaker lines have equivalent widths that are comparable to other M giants of similar temperature; however, the stronger lines of all species are noticeably enhanced in HR 2508. In order to be

TABLE 10

^{14}NH FUNDAMENTAL VIBRATION-ROTATION LINES

LINE	σ (cm^{-1})	χ (eV)	log gf P_1	P_2	P_3	$W_\sigma(cm^{-1}) \times 10^3$ ρ Per	HR 1105	μ Gem	HR 2508	ω Vir	10 Dra	HR 7442	HR 8062
1–0 Band													
*P*15.....	2522.8	0.47	−4.89	−4.91	−4.95	8	8	7	10	12	10	...	11
*P*13.....	2615.0	0.36	−4.85	−4.88	−4.92	8	13	9	9	16	14	15	14
*P*12.....	2659.9	0.31	−4.84	−4.87	−4.91	16	13	11	15	23	12	17	11
2–1 Band													
*P*12.....	2519.1	0.69	−4.34	−4.37	−4.41	9	...	11	12	10	8	18	15
*P*10.....	2604.0	0.60	−4.34	−4.38	−4.43	13	15	13	18	12	14	15	18
*P*9.....	2645.3	0.56	−4.34	−4.38	−4.44	16	18	16	20	23	17	15	16
*P*8.....	2685.5	0.53	−4.35	−4.39	−4.46	20	16	16	19	24	14	20	18

TABLE 11

STELLAR ABUNDANCES[a]

Element	ρ Per	HR 1105[b]	μ Gem	HR 2508[b]	RS Cnc[b]	44 Leo[b]	ω Vir	10 Dra[b]	α Vul	HR 7442[b]	HR 8062[b]	HR 8714[b]
^{12}C	8.48 ± 0.05	8.73 ± 0.10	8.49 ± 0.07	8.28 ± 0.11	8.60 ± 0.09	8.44 ± 0.07	8.49 ± 009	8.51 ± 0.07	8.52 ± 0.08	8.41 ± 0.05	8.70 ± 0.09	8.83 ± 0.04
$^{12}C/^{13}C$	16	34	15	18	35	12	16	10	7	25	46	63
^{14}N	8.33 ± 0.18	8.40 ± 0.11	8.32 ± 0.08	8.54 ± 0.10	8.70 ± 0.13	8.38 ± 0.08	8.60 ± 0.12	8.45 ± 0.15	8.31 ± 0.09	8.44 ± 0.17	8.44 ± 0.16	8.61 ± 0.17
^{16}O	8.93 ± 0.15	8.92 ± 0.05	8.85 ± 0.12	8.80 ± 0.06	...	...	8.81 ± 0.06	9.00 ± 0.09	8.97 ± 0.06	8.94 ± 0.12	8.84 ± 0.16	9.02 ± 0.04
[Ti/H][c]	-0.08 ± 0.14	$+0.01 \pm 0.19$	$+0.15 \pm 0.14$	$+0.04 \pm 0.24$	-0.25 ± 0.11	-0.08 ± 0.15	-0.00 ± 0.20	$+0.23 \pm 0.25$	-0.17 ± 0.08	$+0.06 \pm 0.15$	$+0.12 \pm 0.14$	$+0.01 \pm 0.26$
[Fe/H]	$+0.05 \pm 0.17$	-0.01 ± 0.16	$+0.11 \pm 0.14$	$+0.17 \pm 0.19$	$+0.09 \pm 0.07$	$+0.11 \pm 0.14$	$+0.12 \pm 0.24$	-0.04 ± 0.20	-0.18 ± 0.10	$+0.12 \pm 0.20$	$+0.16 \pm 0.11$	-0.02 ± 0.19
[Ni/H]	-0.27 ± 0.12	-0.20 ± 0.14	-0.05 ± 0.10	$+0.10 \pm 0.16$	-0.36 ± 0.09	-0.02 ± 0.14	-0.10 ± 0.22	-0.17 ± 0.16	-0.14 ± 0.14[c]	-0.05 ± 0.21	-0.10 ± 0.14	-0.21 ± 0.08
[Sr/H]	+0.26	+1.16	+0.32	+0.95	+1.13	+0.20	+0.39	+0.58	...	+0.80	+1.13	+1.00
[Y/H]	−0.32	+0.80	−0.12	+0.25	+0.64	+0.05	+0.00	−0.28	−0.23	−0.09	+0.43	+0.45
[Zr/H]	-0.27 ± 0.14	$+0.64 \pm 0.11$	-0.06 ± 0.20	-0.07 ± 0.08	$+0.65 \pm 0.22$	-0.06 ± 0.11	-0.14 ± 0.17	-0.21 ± 0.17	-0.28 ± 0.07	-0.05 ± 0.18	$+0.38 \pm 0.15$	$+0.36 \pm 0.10$
[Ba/H]	−0.10	+0.61	+0.05	...	+0.35	+0.06	−0.23	−0.11	+0.02	−0.07	+0.10	+0.20
[Nd/H]	+0.14	+0.68	+0.21	+0.22	+0.57	+0.24	−0.01	−0.01	+0.08	+0.15	+0.36	+0.37

[a] Absolute abundances are scaled to log ϵ(H) = 12.0. In this scale, the solar CNO abundances are log ϵ(C) = 8.67, log ϵ(N) = 7.99, log ϵ(O) = 8.92 (Lambert 1978).

[b] Classified as MS or S (Yamashita 1967).

[c] All bracketed abundances are relative to α Tau.

certain that one is detecting true differences in stars, variations in properties of the stellar atmosphere must be considered over and above those considered in spectral classification.

Yamashita (1967) lists 11 stars as type MS in his magnitude-limited sample of M, MS, and S stars. With the three stars from Paper I and the six in this study, we have analyzed nine of Yamashita's candidates. Out of these nine, we find that four show no definite evidence of *s*-process enhancement. In addition, some data are available for the other two stars out of the 11, ST Her and HR 2967. The observations of ST Her reveal an extremely crowded spectrum with broad, blended lines and an apparent weakening of the line depths suggestive of a veil of emission filling in the features. Although no quantitative analysis was attempted on this star, the Zr I, Y II, and Nd II lines are observed to be enhanced relative to the Fe-peak lines suggesting that ST Her belongs to (i.e., it probably shows enhancements of the *s*-process elements) the MS-star group. McDonald near-IR spectra are available for HR 2967, but no FTS spectra are available; thus it has not been included in our sample. An examination of its spectrum shows normal *s*-process lines, hence, it probably does not show enhancements of the heavy elements. The net break-down of Yamashita's MS stars is that six out of 11 shows evidence of the *s*-process and five do not. Although we are in no position to provide spectral classifications, we shall, for the remainder of the paper, label only those stars with definite *s*-process enhancements as MS, and consider the four other stars (HR 2508, 44 Leo, 10 Dra, and HR 7442) to be normal M giants (this relabeling is supported by the C, N, and O abundances to be discussed in § IV). In addition, we find that the extreme ^{12}C-abundances found for HR 363 (Paper I) are more typical of the S-stars, HR 1105 and HR 8714, so we consider it to be of type S rather than MS (this reclassification is also suggested by the very large $^{16}O/^{17}O$ and $^{16}O/^{18}O$ ratios found in these three stars by Harris, Lambert, and Smith 1985). In summary, we find seven stars that show definite heavy-element excesses and we subdivide these as MS (RS Cnc and HR 8062 with o^1 Ori and HR 6702 from Paper I) and S (HR 1105 and HR 8714 with HR 363 from Paper I).

Spectra at 4250 Å were obtained for six out of the seven MS/S stars, the exception being RS Cnc for which a spectrum is available in the literature (Sanner 1978). Three M giants were also observed: ρ Per plus β Peg and 30 Her from Paper I. Since this region is extremely crowded with lines, a spectrum synthesis was deemed appropriate. Of the three Tc I lines, the 4262.24 Å is the least blended. Garstang (1981) has published theoretical *gf*-values for transitions arising from the a^6S ground state of Tc I, and we adopt his value of $gf = 0.59$ for the 4262 Å line. The 4238.19 Å Tc I line is deep within the wing of the Ca I resonance line (4226.173 Å), and the 4297.06 Å line is blended with a strong Cr I line. In spite of the blending, these Tc I lines are obviously present in those spectra in which the 4262Å line is present. The region from 4253–4265 Å was synthesized. The atomic lines in this region were measured in the Sun and solar *gf*-values computed. Additional atomic lines not visible in the solar spectrum were included from the compilation of Kurucz and Peytremann (1975). This region also contains CH whose wavelengths, *gf*-values, and excitation potentials were provided by Brown (1985).

In a similar analysis of Tc I lines in Mira variables, Dominy and Wallerstein (1986) point out that for ^{99}Tc, with a nuclear spin of $I = 9/2$, lines will be split into several hyperfine (hfs) components. The hfs structure of the 4262 Å line has been measured (Wendlandt, Bauche, and Luc 1977). We assigned relative intensities according to the scheme of *LS* coupling (here, more appropriately, *JI* coupling)—see White (1934). It is important to take account of the hfs of the Tc I lines; for an MS or S star with a technetium abundance equal to what might be expected from a recent *s*-process dredge-up, neglect of hfs in the 4262 Å line leads to an overestimate of the abundance by 0.5–0.7 dex.

The observations of the MgH $Q_1(22)$ and $R_1(10)$ lines of the (0, 0) band of the $A\ ^2\Pi$–$X\ ^2\Sigma$ system near 5140 Å were used to estimate Mg-isotopic abundances in two normal M giants, β Peg and ρ Per, and three stars showing enhanced *s*-process abundances, HR 363, o^1 Ori and HR 8062. These two lines are relatively unblended; the (1–1) $R_2(4)$ line is blended with the $R_1(10)$ line. The spectral region from 5138–5141 Å, which covers both MgH lines, was synthesized with atomic lines included from the Sun (with solar *gf*-values) and the Kurucz and Peytremann (1975) listing. Wavelengths, *gf*-values, and excitation potentials for the MgH lines were taken from Lambert and McWilliam (1986). Direct comparison of MgH profiles in M, MS, and S stars suggests that ^{25}Mg and ^{26}Mg are not enhanced in the *s*-process enriched stars (see Clegg, Lambert, and Bell 1980).

IV. DISCUSSION

a) *Introduction*

In this section we discuss the results obtained from the entire sample of late-type giants (both Paper I and this study) in the following order: (1) the Fe-peak elements, (2) the C, N, and O abundances, (3) the *s*-process elements, (4) technetium as an age indicator, and (5) the magnesium isotopic ratios as a signature of the neutron source ^{22}Ne(α, n)^{25}Mg.

b) *The Iron Peak*

Pooling the results from Table 5 in Paper I and Table 11 from this study, we present abundances for Fe, Ni, and Ti in Figure 5. As non–LTE effects in low-excitation, neutral lines are seen in late-type giants (Ruland *et al.* 1980; Brown, Tomkin, and Lambert 1983; Tomkin and Lambert 1983), we examine our abundances as a function of $T_{\rm eff}$. No trend is seen for [Fe/H] as a function of $T_{\rm eff}$. The stars are all members of the disk population and the spread from $-0.2 \lesssim$ [Fe/H] $\lesssim +0.2$ is a result of uncertainties in the observations and analyses plus real differences in [Fe/H]. Our standard star, α Tau, is set to [Fe/H] = 0.0 and has $T_{\rm eff}$ = 3850 K which is indicated by the cross in Figure 5. The Fe-lines used here arise from fairly high excitation ($\chi \approx 4$–5 eV) moderately weak Fe I lines. The non–LTE effects seen in red giants tend to appear for low-excitation neutral species, and apparently the high-excitation Fe I lines in our study are, to a good approximation, immune to such trends down to temperatures just over 600 K cooler than α Tau.

The noncorrelation of [Fe/H] with $T_{\rm eff}$ provides comforting evidence that the near-IR regions selected for analysis are unaffected by severe TiO blanketing of the continuum. The TiO bands increase dramatically in strength toward lower temperatures and, if such blanketing were masking the continuum, the derived Fe-abundances would decrease with decreasing temperatures. The high-resolution analysis confirms what is apparent from spectrophotometry; namely, that for non-Mira variables down to types as late as M6, there exist near-IR "windows" relatively free of molecular absorption.

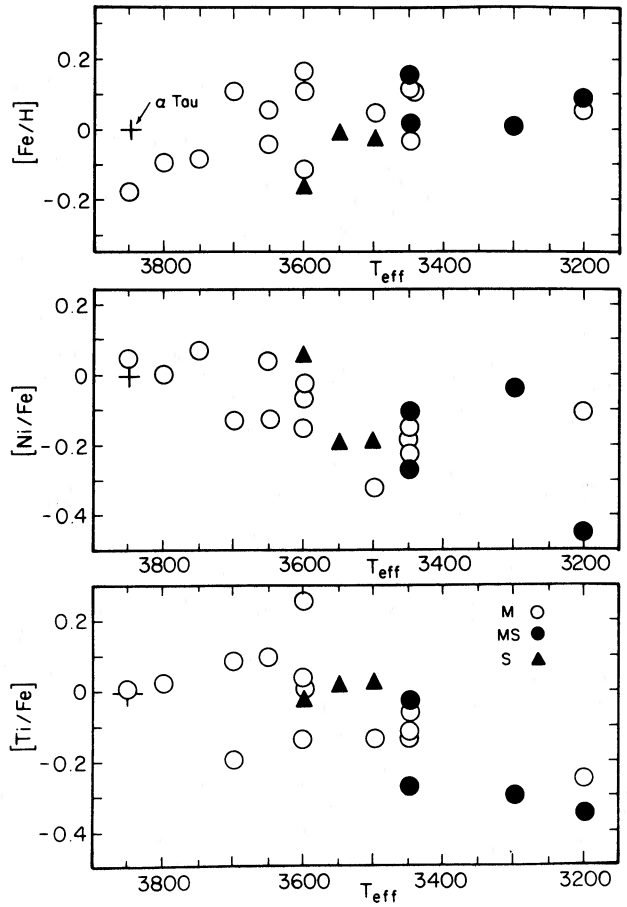

FIG. 5.—Iron-peak abundances, relative to α Tau, as functions of effective temperature for the 12 stars in this paper and nine stars from Paper I.

For both [Ni/Fe] and [Ti/Fe], a similar trend with T_{eff} is evident: [el/Fe] decreases with decreasing temperature reaching [el/Fe] ≈ -0.3 dex near $T_{eff} = 3200$ K. An examination of Table 3 (Table 2 in Paper I) reveals that the Ni I and Ti I lines arise from levels of lower excitation energy ($\chi = 3.3$ eV for Ni I and $\chi = 2.0$ eV for Ti I) and the Ni I lines are typically quite strong. Lower excitation energies and increased line strengths result in the line contribution function being shifted to higher layers of the atmosphere. As discussed by Ruland *et al.* (1980), the assumption of LTE is most likely to break down in the higher layers of a giant's atmosphere where densities become low, hence collisional coupling weakens, and overionization, resulting from the radiation field from deeper layers, becomes important.

c) *Carbon, Nitrogen, and Oxygen*

The vibronic levels of the electronic molecular ground states should be in near LTE (Thompson 1973; Hinkle and Lambert 1975) for these stars, with only small departures expected for the CN red-system lines (Lambert *et al.* 1984). Examination of the [O/H] abundances in Table 11 (Table 5 in Paper I) reveals no trend with T_{eff} even though OH is the most temperature sensitive molecule used in the study. Oxygen is useful in this test as its abundance is not predicted to change during a star's first ascent of the giant branch, whereas carbon and nitrogen will be altered depending upon the extent of the first dredge-up.

Analyses of both NH and CN provide two sets of nitrogen abundances, and a comparison is made in Table 12 for the six stars for which both 2.2 μm and 4 μm spectra exist. The agreement between CN and NH is excellent, and the uncertainties quoted are the internal standard deviations derived from the line-to-line scatter. Lambert *et al.* (1984) found that the N-abundance in α Ori from CN lines was 0.25 dex less than that given by NH. The difference $\log \epsilon\,(N)_{CN} - \log \epsilon\,(N)_{NH}$ in Table 12 ranges from -0.13 to $+0.08$ dex with a mean value of -0.03 dex. Since the CN dissociation energy is an apparent source of a systematic error, we are tempted to conclude that our adopted value [D_0^0(CN) = 7.60 eV] cannot be seriously in error; for example, the value D_0^0(CN) = 7.93 eV claimed by Colket (1984) would reduce the CN-based N abundances by $\sim$0.5 dex. While our adopted dissociation energy D_0^0(NH) = 3.46 eV has been challenged recently, the range suggested by Hofzumahaus and Stuhl (1985), $3.29 < D_0^0(\mathrm{NH}) < 3.46$ eV, would result in higher N abundances from NH lines and so increase the N abundance difference from CN and NH lines.

Quantities related to the C, N, and O abundances are listed in Table 13 (Table 10 in Paper I) and histograms compiled from all 22 stars (including α Tau; although it is technically a K5 III, its C, N, and O abundances are typical of the M stars) are presented in Figure 6. Figure 6 shows that, in the sample as a whole, the ^{16}O abundance scatters about [^{16}O/Fe] = 0.0; as theory predicts, the dredge-up on the first and second ascents of the giant branch have not altered the oxygen abundance. The S stars may possibly be slightly enriched in oxygen. However, we should note that the abundances adopted in the construction of the model atmospheres and those derived in this analysis are not self-consistent. When atmospheres constructed for a carbon-rich mixture typical of S stars are used, their O abundance is decreased by 0.05–0.10 dex such that [O/Fe] for the S stars is brought closer to the value provided by the M stars. A set of model atmospheres with different C/O ratios over a wide range of temperature and gravity is not available in the literature. A set of models with the C/O ratio in the range $0.6 \leq \mathrm{C/O} \leq 1.0$ for a representative temperature and gravity ($T_{eff} = 3500$ K, $\log g = 1.0$) was kindly provided by Dr. Hollis Johnson and his group at Indiana and was used to test the sensitivities of molecular species to the C/O ratio.

The other molecules analyzed, CO, CN, and NH, are much less sensitive to the C/O ratio of the model atmosphere. Varying the C/O ratio of a a sample model atmosphere in the same manner as was done for OH led to the following maximum differences in derived abundances (for typical lines of each molecule) of 0.03 in C from CO, 0.01 in N from CN, and 0.04 in N from NH. Such differences are not significant.

The molecular equilibrium of OH is naturally sensitive to the C/O ratio due to the fact that, since CO is such a tightly

TABLE 12

NITROGEN ABUNDANCES FROM CN AND NH

	$\log \epsilon$ (^{14}N) DERIVED FROM	
STAR	CN	NH
HR 1105	8.35 ± 0.12	8.44 ± 0.10
HR 2508	8.48 ± 0.07	8.61 ± 0.14
ω Vir	8.58 ± 0.10	8.63 ± 0.21
10 Dra	8.49 ± 0.14	8.41 ± 0.19
HR 7442	8.40 ± 0.12	8.48 ± 0.21
HR 8062	8.48 ± 0.12	8.39 ± 0.20

TABLE 13

C, N, AND O ABUNDANCES

Star	[Fe/H][a]	[^{12}C/Fe]	[^{14}N/Fe]	[^{16}O/Fe]	[C+N+O/Fe]	C/O
ρ Per	−0.08	−0.11	+0.42	+0.05	+0.05	0.38
HR 1105[b]	−0.09	+0.15	+0.50	+0.05	+0.13	0.66
μ Gem	+0.04	−0.22	+0.29	−0.09	−0.08	0.47
HR 2508	+0.14	−0.53	+0.41	−0.19	−0.17	0.32
RS Cnc[b]	−0.08	+0.01	+0.79	...	...	...
44 Leo	+0.05	−0.28	+0.34	...	...	...
ω Vir	+0.02	−0.20	+0.59	−0.12	−0.03	0.51
10 Dra	−0.10	−0.06	+0.56	+0.13	+0.13	0.36
α Vul	−0.16	+0.01	+0.48	+0.13	+0.14	0.41
HR 7442	+0.04	−0.30	+0.41	+0.00	−0.02	0.31
HR 8062[b]	+0.05	−0.02	+0.40	−0.11	−0.01	0.74
HR 8714[b]	−0.10	+0.26	+0.72	+0.15	+0.25	0.66

[a] This is the mean of the Fe and Ni abundances.
[b] Stars which show definite *s*-process enhancements.

bound molecule, OH samples the (O–C) abundance. As C/O increases, there will be less available oxygen and near a C/O ratio of unity, the (O–C), or O × (1 − C/O), will become small with the result that small changes in molecular equilibrium (such as slightly different temperature stratifications in models of different C/O ratios) will affect the formation of OH while not significantly altering the formation of more abundant species. Thus, it is useful to compare the derived C/O (C = ^{12}C + ^{13}C) ratios listed in Table 13 (Table 10 in Paper I).

As a sample, the M stars have a mean C/O = 0.45, while the three MS stars (minus RS Cnc for which no O abundance is available) have C/O = 0.64, and the three S stars also have C/O = 0.64. However, as discussed above, the oxygen abundances in the S stars are artificially high by a small amount due to the use of model atmospheres with solar C/O ratios. If the O abundances in the S stars are reduced by 0.1 dex, the resultant mean S-star ratio would be C/O = 0.81. This indicates a real increase in C/O from M to MS to S.

In the M giants, ^{12}C has been depleted and ^{14}N enhanced (i.e., [N/Fe] > 0.0) as is expected during the first dredge-up. The three S stars stand out in terms of their ^{12}C abundances. For the M and MS stars the mean carbon 12 abundance is [^{12}C/Fe] = −0.16 (i.e., [C/Fe] < 0.0), while for the three S stars, it is [^{12}C/Fe] = +0.20. A comparison of the ^{12}C and ^{14}N abundance is shown in Figure 7. The solid curve depicts the result of adding material that has experienced the CN cycle

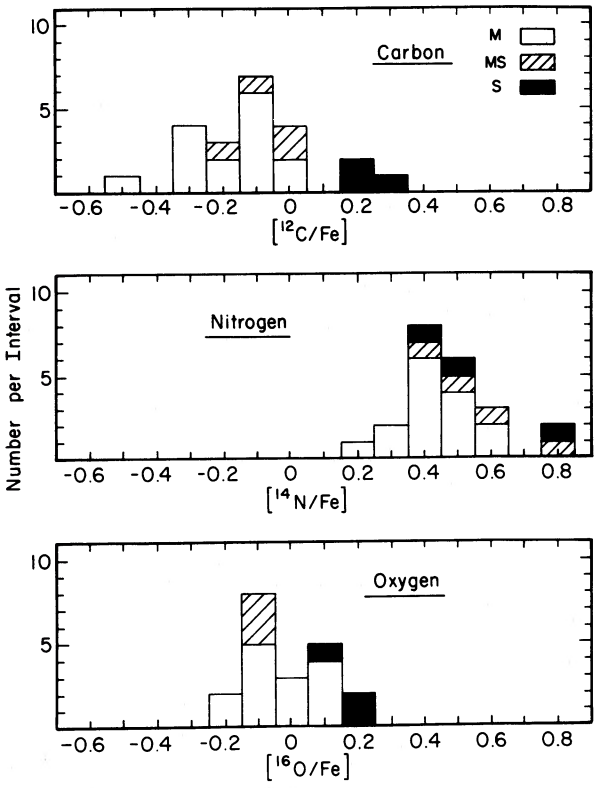

FIG. 6

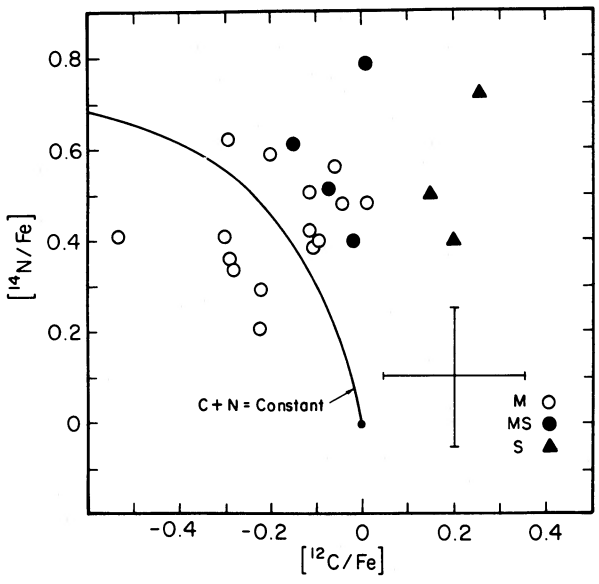

FIG. 7

FIG. 6.—Frequency distribution for the CNO abundances in the 12 stars in this paper and 10 stars from Paper I (α Tau is included with the M stars).

FIG. 7.—The ^{12}C and ^{14}N abundances for the 12 stars in this study and 10 stars from Paper I. Solid line depicts an initial solar ^{12}C and ^{14}N abundance where ^{12}C is then converted to ^{14}N (such as expected from the CN cycle). The error bar represents a typical uncertainty in the [^{12}C/Fe] and [^{14}N/Fe] abundances.

(where ^{12}C is converted into ^{14}N) to an initial solar abundance of ^{12}C and ^{14}N. An error bar representative of the typical uncertainty in the carbon and nitrogen abundances is shown. The M giants scatter about the curve which represents an atmosphere polluted by CN-processed material. The MS stars lie to the ^{12}C-rich side of the distribution represented by the M giants while the S stars are distinguished by their ^{12}C abundance. In Figure 8, ^{12}C abundances are compared to the $^{12}C/^{13}C$ ratios. The M giants form a somewhat tight grouping of points with a mean $^{12}C/^{13}C = 13$. The MS stars show on average larger $^{12}C/^{13}C$ ratios (mean $^{12}C/^{13}C = 30$), with the S star $^{12}C/^{13}C$ ratios being larger still (mean $^{12}C/^{13}C = 38$). As Figure 8 shows, addition of pure ^{12}C to the envelope of an M giant converts the $^{12}C/^{13}C$ ratio to that of the MS and S stars. A naive interpretation of Figures 7 and 8 would be that the S stars are created from M giants through the addition of ^{12}C (from a ^4He burning region). The position of the MS stars in Figure 7 is consistent with the idea that they are less extreme S stars. As noted in Paper I, the C, N, O abundances and $^{12}C/^{13}C$ ratios of M giants match those of the G and K giants.

Two stars, RS Cnc and HR 8714, stand out in terms of their very large nitrogen abundances. For intermediate mass stars ($M \approx 4$–$9\ M_\odot$), a so-called second dredge-up may occur (Becker and Iben 1979) in which the very deep stellar convective envelope sweeps up a large amount of matter where hydrogen has been converted to helium and almost all ^{12}C and ^{16}O have been converted to ^{14}N. Such stars are predicted to exhibit very large overabundances of ^{14}N, such that the nitrogen abundance might rival the oxygen abundance. These two stars may represent stars now on the AGB which experienced a second dredge-up earlier in their evolution.

If we assume that the MS and S stars are created from M giants by dredge-up of ^{12}C following thermal pulses, our abundances require that the ^{12}C abundance in the convective envelope of an M giant must approximately double. A 1 $M_\odot$ star about to begin thermal pulses has a convective envelope mass of about $M_{CE} \approx 0.4\ M_\odot$ (Iben 1983) which, when taken with the mean ^{12}C abundance of $\log \epsilon = 8.5$ for the M giants, leads to $3.0 \times 10^{-3}\ M_\odot$ of ^{12}C in the convective envelope. As Figures 7 and 8 show, the addition of this much more ^{12}C would convert the star to a typical MS-S star. Iben (1983) predicts the amount, M_S, of ^{12}C-rich material dredged up after each thermal pulse for a 1 $M_\odot$ model: M_S varies from $\sim 5 \times 10^{-4}$ to $10^{-3}\ M_\odot$. Thus, a few, say three to six such (theoretical) pulses would create the observed stars from M to MS or S.

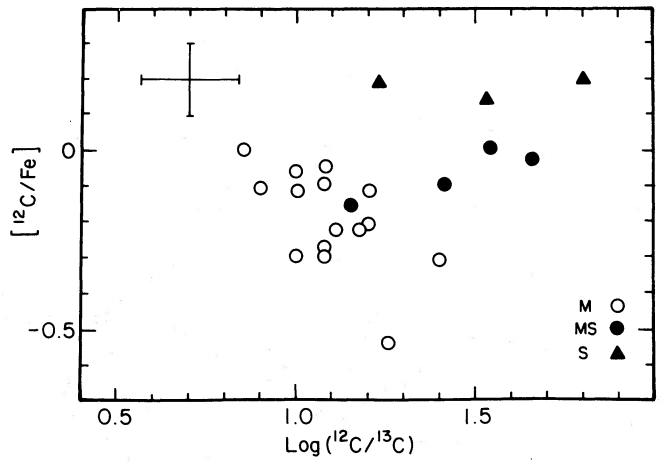

FIG. 8.—Carbon 12 and $^{12}C/^{13}C$ ratios for the 12 stars in this study and 10 stars from Paper I. The typical uncertainties are illustrated by the error bar. The addition of pure ^{12}C to the atmosphere of an M star would be represented by a line from lower left to upper right at an angle of 45°.

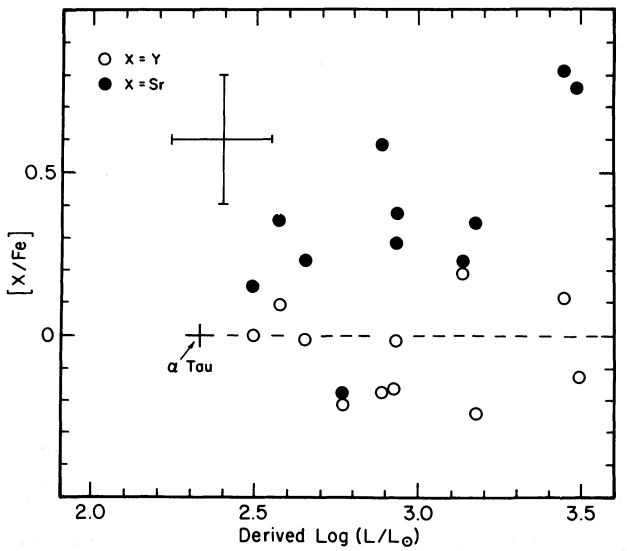

FIG. 9.—The observed trend of the [Sr/Fe] abundance with estimated stellar luminosity (abundances are relative to α Tau). No trend exists for the [Y/Fe] abundance.

We can also use Iben's (1983) predictions to estimate the amount of He-enrichment expected from the above picture. Typically each dredge-up of ^{12}C will include ~ 15 times more ^4He by mass. Thus three to six such injections would increase the mass fraction of ^4He, Y, from an initial value of 0.25 to $\sim$0.30–0.35. This would result in an increase in number abundance from $\log \epsilon\ (^4He) = 10.80$ to $\sim$10.88–10.94. Detecting this slight increase in a cool field giant would be a difficult observational prospect.

d) The s-Process

If we segregate the seven stars which show very definite enhancements of the five heavy elements (Sr, Y, Zr, Ba, and Nd) and the possibly slight *s*-process enriched M giant, 30 Her (Paper I), there remain 13 red giants. We shall first comment on the *s*-process abundances in these stars in which thermal pulses have not operated. The run of the Zr, Y, and Nd abundances with T_{eff} reveals no significant trend; the mean values are [Zr/Fe] = −0.06, [Y/Fe] = −0.08, and [Nd/Fe] to +0.09. A slight trend of [Ba/Fe] is apparent with stars near $T_{eff} = 3400$–3500 down by −0.35 dex relative to the stars with $T_{eff} = 3700$–3800 K. The most striking trend is in the Sr abundances which are enhanced by up to 0.5–0.8 dex in some stars which show no evidence of enhancements in the other *s*-process elements. Although the [Sr/Fe] correlates somewhat with T_{eff}, a much stronger trend is found with the estimated stellar luminosity—see Figure 9 in which 11 stars (plus α Tau) are shown. Two stars (β And from Paper I and α Vul) were not observed in the 10,000 Å region; thus Sr abundances are unavailable. For comparison, we also show in Figure 9 the yttrium abundances; [Y/Fe] is independent of luminosity. Yttrium and strontium are side by side in the periodic table, and the ratio of the Sr/Y abundance produced by the *s*-process is not expected to vary by more than a factor of 2 over a wide

range of neutron exposures ($0.08 \leq \tau_0 \leq 0.6$ mbarn^{-1}; see Cowley and Downs 1980).

Holweger and Kovács (1984) have identified a few K supergiants which apparently have *s*-process enhancements of Ba and Sr only. Such an abundance pattern may be the consequence of a very low neutron exposure ($\tau \lesssim 0.04$ mbarn^{-1}) in which the few available neutrons are captured primarily by odd and relatively abundant nuclei with large neutron-capture cross sections and converted into the magic nuclei ^{88}Sr and ^{138}Ba (Holweger and Kovács 1984). At these low neutron exposures, ^{88}Sr and ^{138}Ba act as bottlenecks to the *s*-process and very few other species are synthesized. A large fraction of the stellar envelope must be exposed to this weak *s*-process, and cycling a substantial part of a star's envelope through such a high temperature as the *s*-process site would be expected to have other observable consequences, such as altered C, N, or O abundances and isotopic ratios, which are not seen in these normal M giants. In short, we discount the possibility that the Sr abundances are the result of *s*-processing.

We discount also the possibility that the Sr trend is traceable to the estimated luminosities, obtained from the Wilson-Bappu Effect, proper motions, or spectral type. An attempt to alter the luminosity, and through that some combination of log g and $T_{\rm eff}$, would also change the other *s*-process and iron group abundances in generally the same sense; Sr would remain an anomaly.

The true culprits behind the high Sr abundances may be the model atmospheres and our assumption of LTE. Typically, the Sr II line was one of the strongest of the *s*-process lines used. The line-core forms in the outermost layers of the model atmosphere where such effects as overionization or scattering, or both, could act to increase the line-depth. Auman and Woodrow (1975) show that overionization increases very rapidly with decreasing optical depth such that in the MS and S stars, the Sr II line may be formed too high in the atmosphere to be a reliable abundance indicator. The Y II line, on the other hand, is much weaker and forms in deeper layers where LTE is shown to be a better approximation (Auman and Woodrow 1975). Abundances derived from this strong Sr II line in very cool giants need to be checked carefully, and in some cases, rejected.

Abundance patterns for four stars are shown in Figure 10: μ Gem is a typical M giant, 44 Leo is one of the stars classified as MS by Yamashita (1967) but showing no significant *s*-process enhancement, while RS Cnc is a true MS star and HR 1105 an S star. As shown above, ^{12}C is a distinguishing characteristic of true MS and S stars. Figure 11 shows that the *s*-process and ^{12}C enhancements are well correlated: [*s*/Fe] in Figure 11 is defined as the mean of [Y/Fe] and [Nd/Fe] because such ratios are reliably derived from weak, singly ionized lines and the pair represents both a "light" and a "heavy" *s*-process element. The correlation strongly suggests that the site of the *s*-process is on or near the ^{4}He-burning shell in which the ^{12}C is synthesized.

It is of interest to use the *s*-process enhancement to estimate the total amount of material that has been cycled through the ^{4}He-burning layers and subsequently mixed into the convective envelope. By the time that the ^{12}C/Fe ratio has been increased by a factor of 2 over that seen in the M giants, the *s*/Fe ratio has increased by about a factor of 4 (about +0.6 dex). If we assume that the initial heavy-element abundance distribution was solar, a 1 $M_\odot$ AGB star with a 0.4 $M_\odot$ convective envelope (Iben 1983) would require the addition of 2.4×10^{-8} $M_\odot$ of pure Y and Nd to obtain a factor of 4

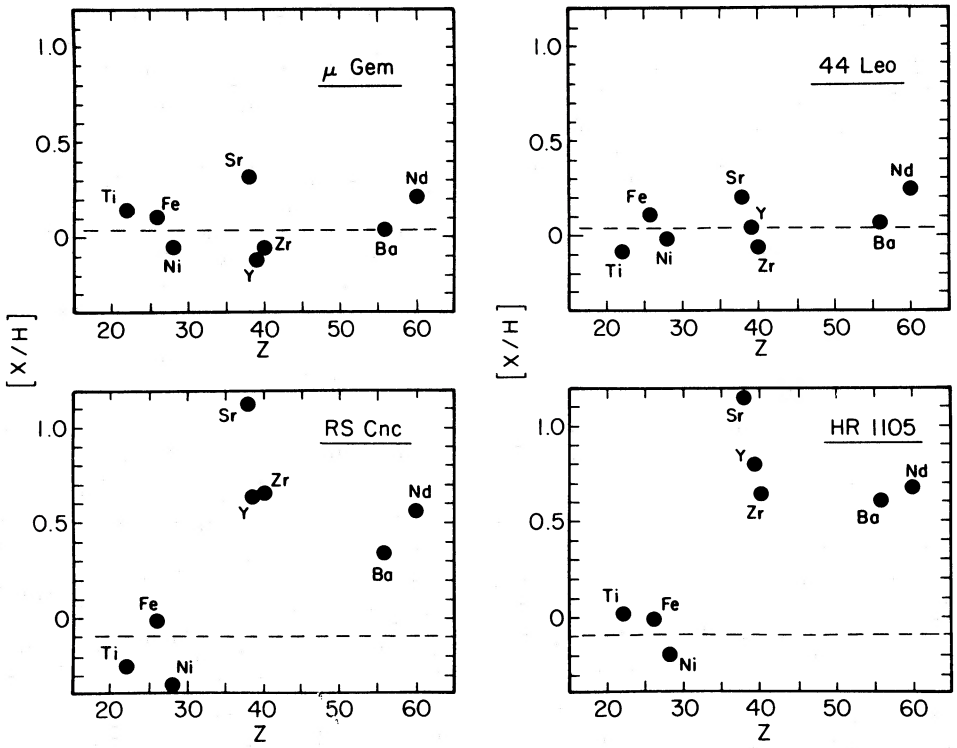

FIG. 10.—Abundances of the heavy elements in four red giants. Mu Gem is a normal M star, while 44 Leo is classified MS yet shows normal (within the errors) *s*-process abundances. Both RS Cnc (MS) and HR 1105 (S) show large enhancements of the *s*-process elements.

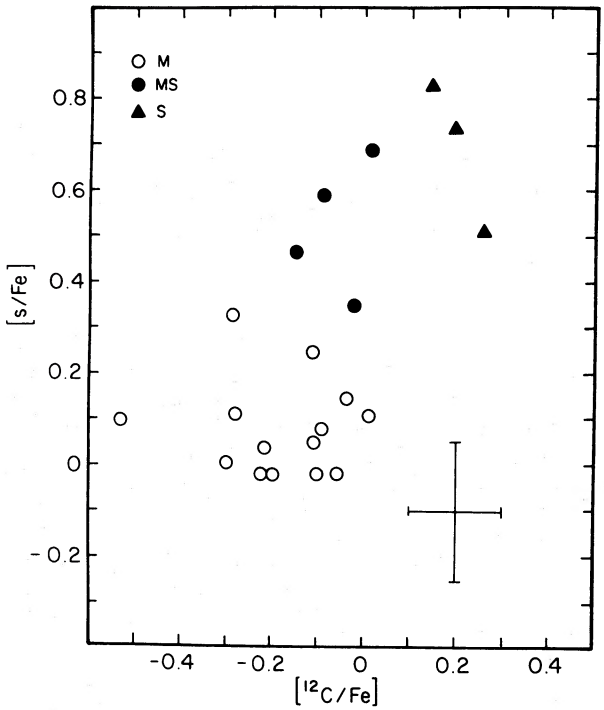

FIG. 11.—The abundance of the *s*-process elements and carbon 12 in the M, MS, and S stars. The [s/Fe] abundances are relative to α Tau and are the average of the [Y/Fe] and [Nd/Fe] abundances. All stars from this study and Paper I are included. Typical uncertainties are illustrated by the error bar.

enhancement. From the predicted abundances (Cowley and Downs 1980), which reproduce the observed abundance patterns quite well (see below), one can easily estimate that the amount of Fe exposed to neutron captures and synthesized into heavier elements is $\sim 2 \times 10^{-6}\ M_\odot$. For an initial solar abundance of Fe [(log N(Fe)/N(H) = −4.4], this corresponds to a total of $\sim 0.05\ M_\odot$ of material exposed at the *s*-process site. The *s*-process is believed to occur in the convective shell between the carbon-oxygen core and hydrogen-rich shell, and an analytic expression for the mass contained in this shell, as a function of core mass, is given by Iben and Truran (1978). For our low-mass ($1\ M_\odot$) test star, a core mass of $\sim 0.6\ M_\odot$ (Iben 1983) leads to a mass of $0.02\ M_\odot$ contained in the convective shell during a pulse. Thus, to generate the observed *s*-process abundances would require two to three such pulses. This crude estimate is in quite reasonable agreement with our earlier estimate of three to six pulses based upon ^{12}C abundances in S stars. The observed ^{12}C and *s*-process abundances are in rough quantitative agreement with predictions based upon low-mass, third dredge-up models that have experienced a few to half-a-dozen thermal pulses.

The abundance pattern for the *s*-process elements can give information on the cumulative neutron exposure and the source of neutrons; a large neutron exposure will produce relatively more of the heavier *s*-process isotopes (i.e., more Nd and Ba relative to Zr, Y and Sr). The most likely sources of neutrons to drive the *s*-process are $^{22}Ne(\alpha, n)^{25}Mg$ and $^{13}C(\alpha, n)^{16}O$. The ^{22}Ne source requires a higher temperature ($T \approx 3 \times 10^8$ K) than the ^{13}C source ($T \approx 10^8$ K) and has been associated with AGB evolution in intermediate mass ($M \gtrsim 5\ M_\odot$) stars (Iben 1975).

The tabulated *s*-process predictions from Cowley and Downs (1980) are used to obtain a fit to the observed abundances, N^s_{el}, in the four MS and three S stars. The observed abundances are a mixture of initial envelope and *s*-processed material. A simple scheme for obtaining the true composition of the *s*-processed material is provided by Tomkin and Lambert (1983):

$$N^s_{el} \propto (y - 1)N^{std}_{el} ,$$

where

$$y = (N^{AGB}_{el}/N^{AGB}_{Fe})/(N^{std}_{el}/N^{std}_{Fe}) \quad \text{with} \quad N^{obj}_{el} ,$$

representing the number density of atoms of element "el" in the object "obj" (AGB = MS or S star and std = α Tau). The abundances from Table 11 provide *y* since log *y* = [el/Fe], and we assume that the abundance distribution of the heavy elements in the standard star, α Tau, is the same as the Sun.

The tabulated predictions produced by an exponential distribution function of neutron exposures, $N(\tau) \propto \exp(-\tau/\tau_0)$, were used to fit observed abundances to a particular exposure parameter, τ_0. This mixture of light and heavy exposures may simulate what occurs in real AGB stars where material could suffer a variety of exposures. Also, very good fits to τ_0 distributions have been obtained for the *s*-process elements in barium stars (Tomkin and Lambert 1983; Smith 1984) and subgiant CH-stars (Krishnaswamy and Sneden 1985). Our selection of elements is limited, and we reject the Sr abundance based upon the Sr II line, which suffers from large systematic trends, and the Ba abundances from the very weak Ba I line which is subject to some blending. The remaining two light *s*-process elements (Y and Zr) and one heavy *s*-process element (Nd) are well suited for characterizing a neutron exposure. Both of the Y/Nd and Zr/Nd ratios change by over a factor of 100 between $\tau_0 = 0.1$ mbarn^{-1} and $\tau_0 = 0.6$ mbarn^{-1}. Table 14 lists the derived values of τ_0 which characterize the heavy-element distributions. The uncertainties in τ_0 are typically ± 0.04 mbarn^{-1}. There is a significant spread in the values of τ_0, ranging from quite low exposures in o^1 Ori and HR 6702 (both MS stars) to quite high exposures in HR 363 and HR 1105 (both S stars). For comparison, the bulk of the solar-system *s*-process elements heavier than Sr are characterized by $\tau_0 = 0.26$ mbarn^{-1}, while the majority of barium stars analyzed are in the range of $\tau_0 \approx 0.4$–0.6 mbarn^{-1} (Tomkin and Lambert 1983; Smith 1984).

It is apparent that low values of τ_0 are associated with lower abundances of ^{12}C (Fig. 12). The three S stars stand out as having the largest neutron exposures as well as the most ^{12}C in their atmospheres. We speculate that the trend of τ_0 with [^{12}C/Fe] is caused by repeated thermal pulses followed by successive dredge-ups. Each episode of dredge-up will increase the ^{12}C abundance. The increasing values of τ_0 could be the result

TABLE 14

s-PROCESS QUANTITIES

Star	τ_0(mbarn^{-1})	Tc?	log ε (Tc)	log [ε (Tc)/ε (Zr)]
HR 363[a]	0.44	No	$\lesssim -1.0$	$\lesssim -4.2$
o^1 Ori[a]	0.16	Yes	+0.1	−2.6
HR 6702[a]	0.18	Yes	−0.8	−3.4
HR 1105	0.49	No	$\lesssim -1.0$	$\lesssim -4.2$
RS Cnc	0.37	Yes[b]	...	...
HR 8062	0.38	Yes	−0.4	−3.3
HR 8714	0.38	Yes	−0.5	−3.2

[a] Stars from Smith and Lambert 1985 (Paper I).

[b] Tc-detection from Sanner 1978. No abundance estimate.

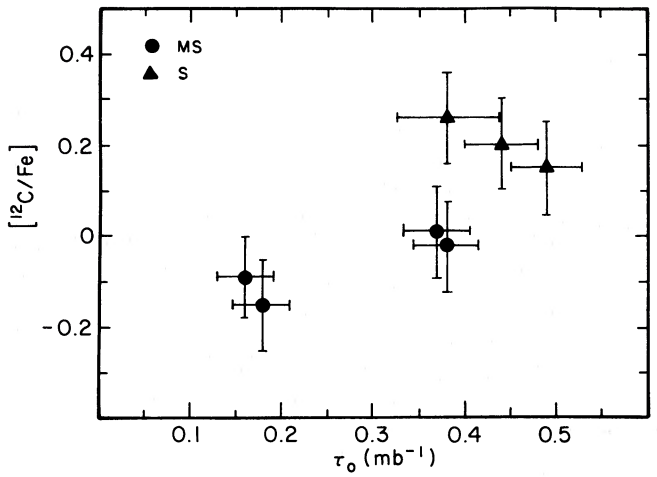

FIG. 12.—The abundance of ^{12}C and the integrated neutron exposure, τ_0, derived from the Y, Zr, and Nd abundances for the MS and S stars. Larger values of τ_0 are associated with larger ^{12}C abundances.

of some fraction of material in the convective shell near the pulse being subjected to repeated *s*-process episodes. This simple picture of repeated processing events was first put forward by Ulrich (1973) as an example in which an exponential distribution of neutron exposures would be appropriate.

e) Technetium as an Age Indicator

The isotope of technetium produced by the *s*-process is ^{99}Tc with a ground-state half-life of 2.13×10^5 yr. The search for the three permitted Tc I resonance lines near 4250 Å proved to be a fruitful one. In two normal M giants, β Peg and ρ Per, and the cool M giant 30 Her, which may show very slight overabundances of Y, Zr, Ba, and Nd (Paper I), no hint of any of the three lines was seen. Of the seven stars showing definite *s*-process enhancements, five showed clear signatures of the three Tc I lines (o^1 Ori, HR 6702, RS Cnc, HR 8062, and HR 8714) while two (HR 363 and HR 1105) did not (see Table 14). This is an interesting observation. Technetium was detected in four out of four MS stars and one out of three S stars.

Technetium, with a half-life of $\sim$200,000 yr, is expected to be detectable in a cool, stellar atmosphere for several half-lives following its production and deposition in the convective envelope. Assuming an initial Tc-abundance equal to that expected from analyses of other *s*-process elements, our synthetic spectra show that the permitted resonance lines should be visible for $\sim$6–7 half-lives (or ~ 1.3–1.5×10^6 yr) in a typical MS or S star. The maximum lifetime of thermally pulsing stars on the AGB is $\sim 2 \times 10^6$ yr (Iben 1983) so the Tc I lines should be visible throughout most of a star's presence on the AGB.

A possible complication concerning technetium is the temperature sensitivity of the half-life of ^{99}Tc due to populating excited levels of the nucleus at temperatures greater than $\sim 10^8$ K (Cameron 1959). The half-life changes from $\sim 2 \times 10^5$ yr at 10^8 K to only 2.5 yr at 3×10^8 K (Cosner and Truran 1981; Schatz 1983)! This fact, along with the presence of Tc abundances near those expected for equilibrium *s*-processing in two SC stars, led Smith and Wallerstein (1983) to suggest that the temperatures in the *s*-process sites in the stars studied by them were not much greater than 10^8 K. Recently, however, Mathews *et al.* (1986) have carried out temperature-dependent *s*-process network calculations and find that the thermally enhanced β-decay rates for ^{99}Tc are nearly compensated by increased neutron production at higher temperatures [they assume a $^{22}Ne(\alpha, n)^{35}Mg$ neutron source]. They find that in most cases ^{99}Tc is produced at near-equilibrium (i.e., no β-decay) values and, at worst, is still at 70% of its expected abundance. Thus, within the accuracies of our analysis, the temperature-sensitive survival of Tc will not be of importance.

The detection of technetium in five out of seven apparent (i.e., *s*-process enhanced) AGB stars supports the above contention concerning the visibility of Tc I, and the conclusion is strengthened by a closer inspection of the two stars not showing Tc I lines. It is possible that the latter pair may be evolved barium stars. Griffin (1984) has shown that one of them, HR 1105, is a single-lined spectroscopic binary. The long-period orbit resembles those observed for the barium stars (McClure 1983). It is becoming increasingly apparent that all barium stars are binaries (McClure, Fletcher, and Nemec 1980; McClure 1983) probably with white-dwarf companions (Böhm-Vitense 1980; Böhm-Vitense, Nemec, and Proffitt 1984). This suggests that the ^{12}C and *s*-process enhancements observed in barium stars, which are too faint and warm to be AGB stars (Scalo 1976), are the result of mass transfer from a former AGB star (now a white dwarf) onto a companion star (now a barium star). The close similarities between the composition of barium and the *s*-process/^{12}C enriched AGB stars of spectral types MS, S, SC, or C is additional evidence for the mass-transfer hypothesis (Lambert 1985). HR 1105 is a candidate to be a cool, luminous member of the barium star class. The absence of Tc is then explained by the long time taken to evolve to the AGB following mass transfer. Supporting evidence is provided by Peery (1985) who inspected archival *IUE* spectra of HR 1105 and deduced the presence of a hot, underluminous companion. The other *s*-process enriched star lacking technetium is HR 363. Although not yet established as a binary, it is listed as a possible spectroscopic binary in the *Bright Star Catalogue* (Hoffleit 1982). Radial velocity studies and UV spectroscopy of this star are in order as it may be similar to HR 1105 and, hence, an evolved barium star.

The remaining five AGB candidates all show Tc and must be currently experiencing, or have just recently experienced ($\lesssim 10^6$ yr), thermal pulses and third dredge-up. A quantitative estimate of the abundance of Tc relative to the other *s*-process elements would be a useful age indicator. As described in § III, synthetic spectra in the region of the 4262 Å Tc I line were computed. This is a very crowded region of the spectrum with the emergent flux of a cool star falling off very rapidly toward shorter wavelengths; hence, model spectra may not reproduce observations very well. Indeed, inspection of representative M giant spectrophotometry from Kiehling and Dachs (1985) reveals that the flux ratio, $F(\lambda = 4250 \text{ Å})/F(\lambda = 10{,}000 \text{ Å})$, is some 30% less in real stars than predicted from the flux distribution of a model atmosphere with similar $T_{\rm eff}$ from Johnson *et al.* (1980); the line blanketing adopted for the models may be reasonably supposed to underestimate the true blanketing. With solar *gf*-values for the atomic lines and our stellar abundances, the synthetic lines near 4250 Å were much too strong to match the observed line depths for β Peg. As the line strength is influenced by the ratio of line to continuous opacity, an underestimate of the continuous opacity in the model will result in a spectral line that is too strong. Omission of densely packed lines simulates an underestimate of the

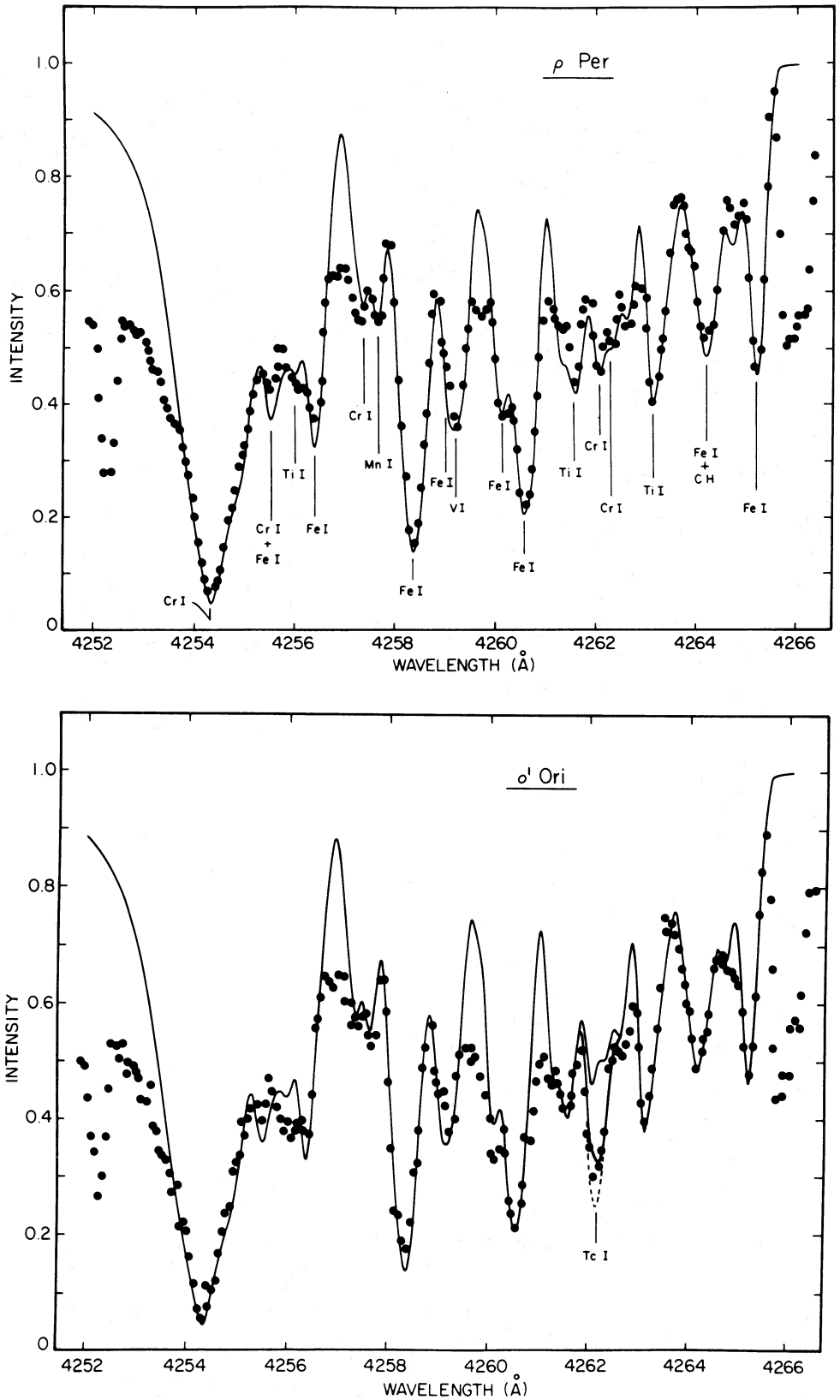

FIG. 13.—Sample synthetic (*solid or dashed lines*) and observed (*dots*) spectra of the region containing the 4262 Å Tc I line. Atomic oscillator strengths were fixed using the normal M star β Peg. Rho Per is a normal M star (no Tc), and a good match is obtained with β Peg *gf*-values. The three syntheses contain varying Tc abundances: (1) no Tc, (2) $\log \epsilon$ (Tc) $= -0.5$, and (3) $\log \epsilon$ (Tc) $= +0.5$ [$\log \epsilon$ (H) $= 12.0$].

(quasi-) continuous opacity. We chose to alter *gf*-values until an acceptable fit was obtained for β Peg. These altered *gf*-values, along with a Tc I *gf*-value adjusted by a similar factor, were then used to synthesize the spectra of MS and S stars, which have similar values of $T_{\rm eff}$ and log g, in order to derive approximate Tc abundances. Although this is a crude method, it approximates a differential analysis. For 12 well-defined lines, for which solar *gf*-values were derived, the oscillator strengths had to be reduced by a factor of 2–5 or an average of a factor of 3 in order to fit the spectrum of β Peg. This reduction factor of 3 was applied to all remaining solar lines, the lines from Kurucz and Peytremann (1975) and, of course, the Tc I line. The resultant overall fit to β Peg is satisfactory. The reduction factor is based on a wide range of species (Fe I, Ti I, Cr I, V I, Mn I) and excitation potential (χ = 0.0–4.0 eV). Since the Tc I line is formed in the same atmospheric layers as the test lines, we think it safe to apply the mean reduction factor to its *gf*-value.

In Figure 13 we show two synthetic spectra; the top one is for the M giant ρ Per, which has no technetium, and the bottom one is the MS star o^1 Ori, which shows well-defined Tc I lines. In the ρ Per spectrum, the principal contributors to the stronger features are noted. Although ρ Per is 100 K cooler in $T_{\rm eff}$ than β Peg and has a somewhat lower value of log g, the fit using the β Peg *gf*-values is acceptable. The position of the "continuum" (i.e., intensity = 1.0) was defined by the highest points across the observed Reticon spectra window, and these points are in agreement with spectra covering a much wider wavelength range (3900–4400 Å) for the same, or similar, stars from Dominy and Wallerstein (1986).

The spectrum of o^1 Ori in Figure 13 shows the Tc I line clearly, and the three synthetic spectra have the following abundances of Tc; (1) no Tc (2) log ϵ (Tc) = -0.5, and (3) log ϵ (Tc) = $+0.5$. The best match to the Tc I line indicates log ϵ (Tc) $\approx$ 0.1. Abundances of Tc in the rest of the *s*-process-enhanced stars are listed in Table 14. No spectrum is available for RS Cnc, although the Tc I lines have been seen by Sanner (1978).

A problem arises in attempting to relate Tc abundances derived here to the other *s*-process elements, since the method used for estimating Tc abundances is different from that used for the other *s*-process species and the wavelength regions are also quite different. To alleviate this problem, we compare the Tc abundances to another *s*-process element, Zr, which is observed in this same spectral region. Three unblended Zr I lines observed in this spectral window were taken from the list provided by Dominy and Wallerstein (1986). The three lines of Zr I are 4213.87 (χ = 0.60 eV), 4239.31 (χ = 0.69 eV), and 4240.35 (χ = 0.60 eV). These lines are visible in β Peg and, as with the synthesis of the Tc I region, *gf*-values were altered to fit the β Peg equivalent widths. Abundances derived from the violet Zr I lines, relative to β Peg, are then derived for each star in which an estimate of the Tc abundance is available. A small systematic trend is apparent between [Zr/H] derived from the violet lines and that derived from the near-IR lines in the sense that the average value of [Zr/H] is 0.2 dex smaller for the violet lines than for the near-IR lines. The source of this trend is unknown, but a comparison of the Tc/Zr ratio using only the violet Zr I lines is the most direct approach and reduces systematic uncertainties.

The Zr abundances can be corrected for the observed mixture of initial envelope abundance and *s*-processed material currently in the convective envelope (see § IV*c*). The ratio of log [ϵ(Tc)/ϵ(Zr)] can be computed [all of the Tc is produced in the thermal pulse(s), and this is tabulated in Table 14]. The predicted abundance ratios from the Cowley and Downs (1980) models are $-2.36 < \log [\epsilon(\mathrm{Tc})/\epsilon(\mathrm{Zr})] < -2.20$ for $0.08 \leq \tau_0 \leq 0.60$ mbarn^{-1}. All of the observed Tc/Zr ratios are considerably smaller than the predicted ratios which could indicate a large systematic effect (unlikely—see above) in all of the Tc abundances or loss of Tc by decay in the stellar atmospheres. The derived Tc abundances, relative to other *s*-process elements, are displayed in Figure 14 for two MS stars, o^1 Ori and HR 8062. The corrected *s*-process abundances are shown by the filled circles, while the solid lines are the appropriate abundance predictions from the *s*-process calculations of Cowley and Downs (1980). Each model is the prediction from the appropriate value of τ_0 derived from the Y/Nd and Zr/Nd ratios. The model abundances near technetium are shown for Mo (Z = 42), Tc (Z = 43), and Ru (Z = 44). Technetium is apparently underabundant relative to its fellow *s*-process species.

Kipper and Kipper (1984) have analyzed the violet Tc I lines by a method similar to the one here. They mention that *gf*-values supplied to them by R. A. Bell are all too large; presumably they also find that synthetic lines in this region are too strong. Also, they make use of the heavily blended 4297 Å Tc I line and note that it yields Tc abundances up to 1.0 dex larger than the 4262 Å line. The only star common to both our study and Kipper and Kipper (1984) is o^1 Ori, for which they derive log ϵ(Tc) = $+2.0$, a value inconsistent with theory (see Fig. 14). We note, however, that rejection of the 4297 Å line would apparently lower their abundance considerably while the inclusion of hfs into their analysis would lower the derived abundance still further. After such corrections, it may be that our and their results are in fair agreement.

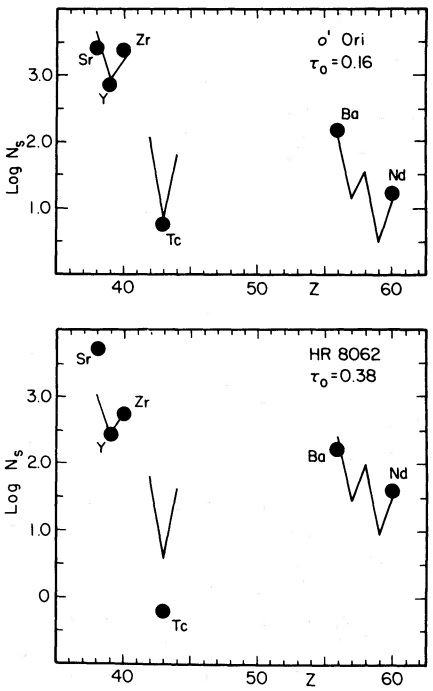

FIG. 14.—Observed *s*-process abundance distributions for two *s*-process enhanced stars (*filled circles*) and model predictions from Cowley and Downs (1980; *solid lines*). The Y, Zr, and Nd abundances were used to fit observations to a particular model.

Quantitative technetium abundances have been estimated for two SC stars (CY Cyg and R CMi) using the intercombination 5924 Å line of Tc I (Smith and Wallerstein 1983). Compared to neighboring *s*-process elements, the abundance was near the *s*-process prediction for CY Cyg and 0.7 dex low in R CMi. Hyperfine splitting was not included in these results so the Tc abundances should probably be reduced by a modest factor. The results of Smith and Wallerstein (1983) are in fair agreement with Tc abundances in the MS and S stars.

Taken at face value, our Tc abundances suggest some decay since injection into the stellar envelope. A quantitative comparison is complicated by repeated pulses and the time between pulses. If the time between pulses, Δt, is short relative to the half-life of ^{99}Tc, $\tau_{1/2}$, then very little Tc would decay during the interpulse period ($\Delta t \ll \tau_{1/2}$) and the amount of Tc decay would represent the time elapsed since pulses and dredge-up began. On the other hand, if $\Delta t \gg \tau_{1/2}$ and Tc suffers significant decay between pulses its abundance will fall below the abundances of stable *s*-process nuclei which are continually built up after each pulse. In a simple picture consisting of identical pulses with equal neutron exposures and the same amount of dredge-up following each pulse, the amount of stable *s*-process elements will increase in direct proportion to pulse number, N. If a substantial fraction of Tc decayed between each pulse, Tc would appear underabundant relative to its *s*-process neighbors by a factor close to N after the nth pulse.

In either picture, the underabundance of Tc results from β-decay following one, or more, thermal pulses and subsequent dredge-ups. Thus, the abundance of technetium can be used to estimate elapsed time as a thermally pulsing AGB star. The underabundances of Tc relative to Zr range from no measurable underabundance for o^1 Ori to 10 for HR 6702 (Table 14) in stars where finite Tc abundances could be estimated. This suggests that HR 6702 has been on the AGB for close to 10^6 yr, and this is in agreement with the expected lifetime of, at most, 2×10^6 yr for a low-mass AGB star (Iben 1983).

f) *Magnesium Isotope Ratios*

The isotopes of Mg should be affected by operation of the ^{22}Ne (α, n)^{25}Mg neutron source, hence, estimates of ^{24}Mg/^{25}Mg and ^{24}Mg/^{26}Mg ratios will shed light on the identity of the neutron source in the AGB stars. Two, largely unblended, MgH lines were synthesized [Q_1(22) at 5138.1 Å and R_1(10) 5139.6 Å] in two M giants (β Peg and ρ Per) and three *s*-process enhanced stars (HR 363, o^1 Ori, and HR 8062). As with the region near 4250 Å, the 5140 Å region is heavily blanketed and the *gf*-values were scaled to match the central depths in each star. The wavelength shift of the isotopic MgH lines is large ($\Delta\lambda \approx 0.15$ Å) and the shapes of the line profiles are sensitive to the isotope ratios. Atomic-line profiles were synthesized to provide the macroturbulent velocity parameter.

Figure 15 illustrates detailed line profiles for two normal M giants and two stars with *s*-process enhancements. In the case

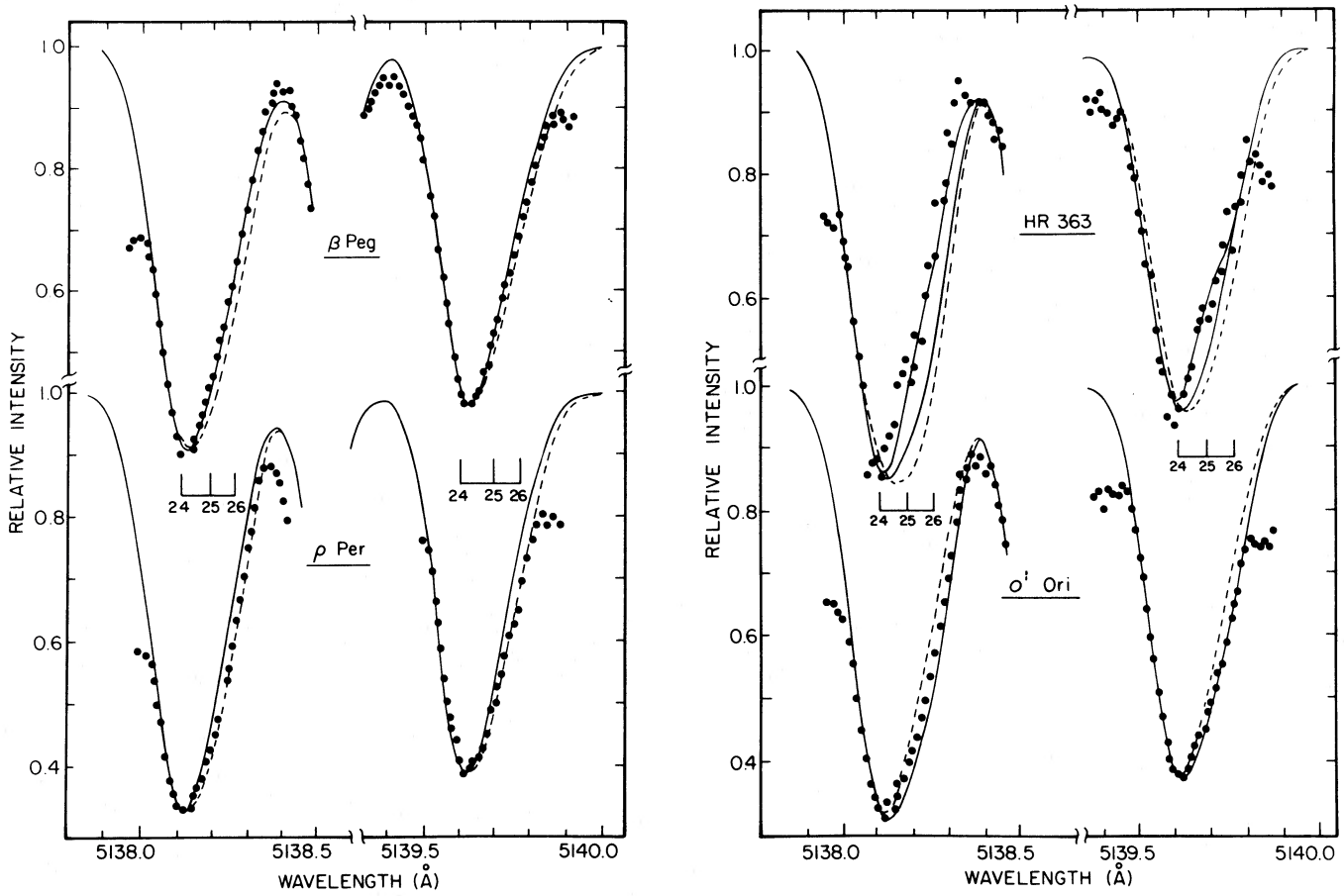

FIG. 15.—Synthetic (*solid or dashed lines*) and observed (*dots*) line-profiles of the two MgH lines used to estimate Mg-isotopic ratios. The two *s*-process enhanced stars (HR 363 and o^1 Ori) are not significantly different from the normal-abundance M stars (β Peg and ρ Per).

of β Peg and ρ Per, the dashed lines represent syntheses with a solar mixture of the Mg isotopes (^{24}Mg:^{25}Mg:^{26}Mg; 79:10:11; Anders and Ebihara 1982) while the solid line is a mix of 90:5:5 and the dots are the observations. A good fit to ρ Per is provided by solar Mg-isotope ratios with β Peg showing slight deficiencies of ^{25}Mg and ^{26}Mg. β Peg is fitted best by a set of isotopic abundances near 87:5:8. The difference in the Mg isotopic ratios is at the observational limit considering the line density in this region and the paucity of "unblended" MgH lines.

Two *s*-process enhanced stars are also shown ion Figure 15; HR 363 and o^1 Ori. These two stars represent extremes of neutron exposure, with o^1 Ori having a very low exposure ($\tau_0 = 0.16$) while HR 363 has a large exposure (0.44 mbarn^{-1}). The two synthetic spectra for o^1 Ori contain a solar mixture of Mg isotopes (*solid line*) and a mixture of 90:5:5. A very slight decrease in ^{25}Mg is suggested, with a good fit to the data being 80: 9:11. The MgH lines in HR 363 indicate a deficiency of ^{25}Mg and ^{26}Mg isotopes relative to the other stars. In Figure 15 for HR 363, the solid line showing the most ^{25}Mg and ^{26}Mg is for a solar isotopic mixture. The other solid lines are for mixtures of 90:3:7 [the $Q_1(22)$ line] and 89:0:11 [the $R_1(10)$ line]. An approximate isotopic breakdown for HR 363 is 88:3:9. The dashed line for HR 363 represents a prediction from Scalo (1978) based upon calculations from Truran and Iben (1977) using the ^{22}Ne(α, n)^{25}Mg neutron source. This represents an isotope mixture having 55:25:20 and is taken from Scalo's (1978) relationship of [*s*-process/Fe] enhancement and the Mg isotopic abundances. Such a ^{25}Mg and ^{26}Mg abundance causes very broad lines and the enriched mixture is obviously not characteristic of HR 363 (or o^1 Ori).

An additional MS star, HR 8062, was observed for MgH and isotopic Mg abundances derived. For HR 8062, the mixture of 82:9:9 was obtained, which is not far off the solar values of 79:10:11. Clegg, Lambert, and Bell (1979) showed that the S star HR 1105 and β Peg had the same isotopic ratios (i.e., approximately a terrestrial mixture).

No enhancement of ^{25}Mg and ^{26}Mg is seen in any of the *s*-process enriched stars, which suggests that ^{22}Ne(α, n)^{25}Mg is not responsible for the *s*-process elements. The competing neutron source, ^{13}C(α, n)^{16}O, is the likely source of neutrons required to drive the *s*-process reactions in the MS and S stars. Since the ^{22}Ne source would be ignited at temperatures above $\sim 3 \times 10^8$ K and would prove adequate to drive significant *s*-processing, we suggest that the temperature at the *s*-process site was below this value but above the ignition temperature for the ^{13}C source ($T \approx 10^8$ K). This requirement suggests that the MS/S stars are of low-mass ($M \lesssim 2\ M_\odot$; Truran and Iben 1977).

V. CONCLUSION

A total of 22 M, MS, and S stars have now been analyzed in this paper and Paper I (including α Tau as a somewhat warmer example of the M giants, i.e., first dredge-up). Our quantitative analysis suggests that about half of Yamashita's (1967) MS stars are indistinguishable from normal M giants by their C, N. O, Fe group, and *s*-process abundances. If our *s*-process enhancements are used to define the spectral classes, our sample consists of 15 M, four MS, and three S stars.

By their chemical composition, the M giants do not differ from typical field G and K giants; i.e., the convective envelopes are contaminated by material exposed lightly to the CN cycle during the main-sequence phase and dredged up in the first ascent of the giant branch. The observable consequences of this first dredge-up include a reduction of the ^{12}C and an enhancement of the ^{14}N abundance, and a reduction of the ^{12}C/^{13}C ratio.

For the seven stars which show definite *s*-process enhancements, a clear positive correlation is seen between ^{12}C abundance and *s*-process abundances, demonstrating that the *s*-process regions are associated with the ^{4}He-burning layers. The carbon and heavy-element abundances are consistent with the predicted composition for low-mass ($M \approx 1\ M_\odot$) AGB models after a few (three to six) thermal pulses and the subsequent (third) dredge-up. Detection of technetium in five of the seven MS/S stars confirms the assignment of the site of nucleosynthesis to the interior of a short-lived ($\lesssim 2 \times 10^6$ yr) AGB star. The low Tc abundances in these five stars, in relation to the other *s*-process elements, suggests a lifetime as a thermally pulsing AGB star of as long as 10^6 yr. This is indicative of low-mass AGB stars (Iben 1983). Two stars without Tc may be cool, luminous counterparts of the G and K type barium stars. The fact that one of the pair is a spectroscopic binary and a hint that the other is also a binary is consistent with our suggested link to the barium stars, all of which are spectroscopic binaries. Technetium present in the AGB star prior to creation of the barium star by mass transfer decays in the long interval before the barium star evolves to the AGB.

A low stellar mass is further indicated by the Mg isotopic ratios. Lack of an enhancement of ^{25}Mg and ^{26}Mg (relative to ^{24}Mg) rules out the ^{22}Ne neutron source as the driver of the *s*-process in these MS/S stars and, hence, excludes the more massive stars as the progenitors of our MS/S stars. We suggest that the *s*-process is driven by the ^{13}C(α, n)^{16}O reaction operating in low-mass ($M \lesssim 2\ M_\odot$) stars.

The neutron exposure (τ_0) increases with the overall *s*-process and ^{12}C enrichments. The theory of pulsed *s*-processing in a He-burning zone followed by partial mixing into the convective envelope predicts these correlations. An alternative model of single *s*-processing events of differing strength cannot be excluded; the weak events producing MS stars and the strongest events leading to S stars.

Our abundance analyses with theoretical guidance provided by recent studies of thermal pulses in AGB stars suggests that the MS and S stars are low-mass AGB stars which have experienced just a few pulses. With an enlarged sample of these stars, it may be possible to detect "quantization" of the *s*-process and ^{12}C enrichments, i.e., the enrichment provided by a single pulse. There are suggestions of such quantization in our results—see, for example, the neutron exposure parameter τ_0 (Fig. 12). However, the MS and S stars are unlikely to be a homogeneous group, and differences in stellar mass, metallicity, and, perhaps, other factors must play some role in determining the thermal pulses, the *s*-processing and the dredge-up and, hence, the surface composition. There is a possibility that one may be able to observe a single pulse supply sufficient additional carbon to change the spectral classification of the star.

With our extensions of quantitative spectroscopy to the AGB stars, observational knowledge of the chemical composition of these stars has outstripped the ability of theoretical descriptions of stellar evolution to predict the compositional changes induced by the third dredge-up in low mass stars. We look forward to fruitful interactions between observers and theoreticians.

Other questions deserving future attention by observers

concern the higher mass stars and the $^{22}Ne(\alpha, n)^{25}Mg$ neutron source. Do such stars undergo third dredge-up of *s*-process material from the ^{22}Ne source? Are the lifetimes of the more massive AGB stars so short that they are not easily observed? Are some of the cool supergiants evolved intermediate-mass stars? Perhaps some of the more luminous members of the LMC ($M_{bol} \lesssim -7$) which appear to lie near the AGB need to be studied in detail to answer questions concerning the evolution of stars more massive than $M \gtrsim 4$–$5\ M_{\odot}$ along the asymptotic giant branch.

We thank J. F. Dominy and G. Wallerstein for helpful conversations, J. Tomkin and K. Hinkle for assistance at the telescope. This research has been supported in part by the National Science Foundation (grant AST 83-16635) and the Robert A. Welch Foundation.

REFERENCES

Anders, E., and Ebihara, M. 1982, *Geochim. Cosmochim. Acta*, **46**, 2363.
Auman, J. R., and Woodrow, J. E. J. 1975, *Ap. J.*, **197**, 163.
Becker, S. A., and Iben, I., Jr. 1979, *Ap. J.*, **232**, 831.
Bernath, P. F. 1985, private communication.
Bessell, M. S., and Wood, P. R. 1984, *Pub. A.S.P.*, **96**, 247.
Bidelman, W. P. 1954, *Mem. Soc. Roy. Sci., Liège*, 4th Ser., **14**, 402.
Boesgaard, A. M. 1970, *Ap. J.*, **161**, 163.
Böhm-Vitense, E. 1980, *Ap. J.*, **239**, L79.
Böhm-Vitense, E., Nemec, J., and Proffitt, C. 1984, *Ap. J.*, **278**, 726.
Brown, J. A. 1985, private communication.
Brown, J. A., Tomkin, J., and Lambert, D. L. 1983, *Ap. J.*, **265**, L93.
Cameron, A. G. W. 1959, *Ap. J.*, **130**, 452.
Clegg, R. E. S., Lambert, D. L., and Bell, R. A. 1979, *Ap. J.*, **234**, 188.
Colket, M. B., III 1984, *J. Quant. Spectrosc. Rad. Transf.*, **31**, 7.
Cosner, K., and Truran, J. W. 1981, *Ap. Space Sci.*, **78**, 85.
Cowley, C. R., and Downs, P. L. 1980, *Ap. J.*, **236**, 648.
Dominy, J. F., and Wallerstein, G. 1986, *Ap. J.*, **310**, 371.
Eggen, O. J. 1972, *Ap. J.*, **177**, 489.
Garstang, R. H. 1981, *Pub. A.S.P.*, **93**, 641.
Griffin, R. F. 1984, *Observatory*, **104**, 224.
Hall, D. N. B., Ridgway, S. T., Bell, R., and Yarborough, J. M. 1978, *Proc. Soc. Photo-Opt. Instrum. Eng.*, **172**, 121.
Harris, M. J., Lambert, D. L., and Smith, V. V. 1985, *Ap. J.*, **299**, 375.
Hinkle, K. H., and Lambert, D. L. 1975, *M.N.R.A.S.*, **170**, 447.
Hoffleit, D. N. 1982, *Bright Star Catalogue* (4th ed.; New Haven: Yale University Observatory).
Hofzumahaus, A., and Stuhl, F. 1985, *J. Chem. Phys.*, **132**, L5.
Holweger, H., and Kóvacs, N. 1985, *Astr. Ap.*, **132**, L5.
Iben, I., Jr. 1983, *Ap. J. (Letters)*, **275**, L65.
———. 1975, *Ap. J.*, **196**, 549.
Iben, I., Jr., and Renzini, A. 1982, *Ap. J.*, **263**, L23.
Iben, I., Jr., and Truran, J. W. 1978, *Ap. J.*, **220**, 980.
Johnson, H. L., Mitchell, R. I., Iriarte, B., and Wisniewski, W. Z. 1966, *Comm. Lunar Planet. Lab.*, **4**, 99.
Johnson, J. R., Bernat, A. P., and Krupp, B. M. 1980, *Ap. J. Suppl.*, **42**, 501.
Keenan, P. C. 1954, *Ap. J.*, **120**, 484.
Kiehling, R., and Dachs, J. 1985, in *Cool Stars with Excesses of Heavy Elements*, ed. C. Jaschek and M. Jaschek (Dordrecht: Reidel), p. 87.
Kipper, T. A., and Kipper, M. A. 1984, *Soviet Astr. Letters*, **10**, 6.
Krishnaswamy, K., and Sneden, C. 1985, *Pub. A.S.P.*, **97**, 407.
Kurucz, R. L., and Peytremann, E. 1975, *Smithsonian Ap. Obs. Spec. Rept.*, No. 362.
Lambert, D. L. 1978, *M.N.R.A.S.*, **182**, 249.
———. 1985, in *Cool Stars with Excesses of Heavy Elements*, ed. C. Jaschek and M. Jaschek (Dordrecht: Reidel), p. 191.
Lambert, D. L., Brown, J. A., Hinkle, K. H., and Johnson, H. R. 1984, *Ap. J.*, **284**, 223.
Lambert, D. L., and McWilliam, A. 1986, *Ap. J.*, **304**, 436.
Mathews, G. J., Takahashi, K., Ward, R. A., and Howard, W. M. 1986, *Ap. J.*, **302**, 410.
McClure, R. D. 1983, *Ap. J.*, **268**, 264.
McClure, R. D., Fletcher, J. M., and Nemec, J. M. 1980, *Ap. J. (Letters)*, **238**, L35.
McWilliam, A., and Lambert, D. L. 1984, *Pub. A.S.P.*, **96**, 882.
Merrill, K. M., and Stein, W. A. 1976, *Pub. A.S.P.*, **88**, 523.
Merrill, P. W. 1922, *Ap. J.*, **56**, 457.
———. 1952, *Ap. J.*, **116**, 21.
Paczyński, B. 1970, *Acta Astr.*, **20**, 47.
Peery, B. F., Jr. 1985, in *Cool Stars with Excesses of Heavy Elements*, ed. C. Jaschek and M. Jaschek (Dordrecht: Reidel), p. 333.
Ridgway, S. T., Joyce, R. R., White, N. M., and Wing, R. F. 1980, *Ap. J.*, **235**, 126.
Ruland, F., Holweger, R., Griffin, R., Griffin, R., and Biehl, D. 1980, *Astr. Ap.*, **92**, 70.
Russell, H. N. 1934, *Ap. J.*, **79**, 317.
Sanner, F. 1978, *Ap. J.*, **219**, 538.
Scalo, J. M. 1976, *Ap. J.*, **206**, 474.
———. 1978, *Ap. J.*, **221**, 627.
Schatz, G. 1983, *Astr. Ap.*, **122**, 327.
Schwarzschild, M., and Härm, R. 1965, *Ap. J.*, **142**, 855.
Smith, V. V. 1984, *Astr. Ap.*, **132**, 326.
Smith, V. V., and Lambert, D. L. 1985, *Ap. J.*, **294**, 326 (Paper I).
Smith, V. V., and Wallerstein, G. 1983, *Ap. J.*, **273**, 742.
Sneden, C. 1974, Ph.D. thesis, University of Texas at Austin.
Sweigart, A. V., and Gross, P. G. 1978, *Ap. J. Suppl.*, **36**, 405.
Thompson, R. I. 1972, *Ap. J.*, **181**, 1039.
Tomkin, J., and Lambert, D. L. 1983, *Ap. J.*, **273**, 722.
Truran, J. W., and Iben, I., Jr. 1977, *Ap. J.*, **216**, 797.
Tsuji, T. 1981, *Astr. Ap.*, **99**, 48.
Ulrich, R. K. 1983, in *Explosive Nucleosynthesis*, ed. D. N. Schramm and W. D. Arnett (Austin: University of Texas), p. 139.
van Dishoeck, E. R. 1985, private communication.
Vogt, S. S., Tull, R. G., and Kelton, P. K. 1978, *Appl. Optics*, **17**, 574.
Wendlandt, D., Bauche, J., and Luc, P. 1977, *J. Phys. B*, **10**, 1989.
White, H. E. 1934, *Introduction to Atomic Spectra* (New York: McGraw-Hill).
Wilson, O. C. 1976, *Ap. J.*, **205**, 823.
Yamashita, Y. 1967, *Pub. Dom. Ap. Obs.*, **13**, 47.

DAVID L. LAMBERT and VERNE V. SMITH: Department of Astronomy, University of Texas, Austin, TX 78712.